

1
2
3
4
5
6
7
8
9
10
11
12
13
14
15
16
17
18
19
20
21
22
23
24
25
26
27
28

**Metagenome-wide measurement of protein synthesis in the human fecal microbiota using
MetaRibo-Seq**

Brayon J. Fremin¹ and Ami S. Bhatt^{1,2*}

¹Department of Genetics, Stanford University, CA, 94305, USA

²Department of Medicine (Hematology), Stanford University, CA, 94305, USA

*Correspondence: asbhatt@stanford.edu

29 **Abstract**

30

31 The healthy human fecal microbiota is too diverse to comprehensively study with the
32 current throughput of proteomic methods. Shotgun sequencing technologies allow for much
33 more comprehensive profiling. Here, we develop and apply MetaRibo-Seq, a method for
34 simultaneous ribosome profiling of multiple taxa within a complex bacterial community. This
35 approach captures taxonomic diversity in fecal samples. As expected, the detected ribosome-
36 bound transcripts are relatively enriched within coding regions and significantly correlate to
37 detectable protein abundances. In a low diversity fecal sample, we show that MetaRibo-Seq is
38 more strongly correlated than metatranscriptomic data to protein abundance. This significant
39 correlation of metatranscriptomics and MetaRibo-Seq with protein levels is maintained, though
40 with decreased strength as taxonomic diversity increases. Finally, we identify genes that are
41 consistently regulated at the translational level across bacterial taxa within fecal communities. In
42 conclusion, MetaRibo-Seq enables comprehensive translational profiling in complex bacterial
43 communities for the first time.

44

45

46

47

48

49

50

51

52

53

54

55

56

57

58

59

60 **Introduction**

61 There is great interest in determining the potential functions of the human fecal microbiota.
62 To date, methods have excelled at describing the taxonomy of such communities; however,
63 assigning and defining functions of the community of bacteria or individual organisms within
64 these communities has been challenging¹. An ideal method to study functions within a complex
65 community would allow simultaneous enumeration of all of the proteins, lipids, and other
66 macromolecules within the mixture. Unfortunately, this is not feasible with current technologies.
67 While 10^2 to 10^4 proteins can be simultaneously quantified with metaproteomics², it is
68 challenging to obtain accurate measurements of the full array of bacterial proteins that likely
69 exist in human fecal samples, estimated to be 10^7 to 10^8 proteins³. Thus, current proteomic
70 methods lack the dynamic range required to comprehensively study the human fecal microbiota⁴.

71 Given the challenges in direct protein measurement and need for databases of protein
72 sequences, some have focused on enumerating the gene content of a community to determine the
73 potential function; indeed, progress has been made in predicting genes present within a
74 metagenome⁵. However, the presence of a gene in a complex bacterial community does not
75 imply that the gene is transcribed or translated. Acknowledging this limitation, recent work has
76 demonstrated that differential transcription of bacterial genes can be used to derive biologically
77 meaningful insights^{6,7,8,9}. Yet, we still have a very limited understanding of regulation occurring
78 post-transcriptionally in the human fecal microbiota.

79 In contrast to transcriptomic profiling, ribosome profiling (Ribo-Seq) is a method that
80 quantifies protein synthesis¹⁰. In eukaryotes, Ribo-Seq generally correlates more strongly to
81 protein abundance than transcriptomics^{11,12,13}; this correlation has not been described in bacteria.
82 Bacterial ribosome profiling studies have been performed in model organisms such as
83 *Escherichia coli* and *Bacillus subtilis*, with minor modifications from the eukaryotic protocols,
84 such as using chloramphenicol to inhibit translation and micrococcal nuclease (MNase) to enrich
85 for ribosome footprints^{13,14,15,16,17}. These methodological modifications enable a high-throughput
86 snapshot of translation, but often compromise the ability to achieve codon-level resolution¹¹.

87 In bacteria, many genes are regulated at the translational level. For example, genes
88 involved in translation itself are known to be regulated at a translational level via feedback
89 mechanisms^{18,19,20,21,22}. Translational regulation is critical for generating proteins at the correct
90 stoichiometry for many protein complexes. For example, the multiprotein complex that forms

91 bacterial ATP synthase has multiple genes whose translation is regulated; the stoichiometry of
92 this complex is best predicted by Ribo-Seq^{13,17}. This even extends to pathway-specific enzyme
93 stoichiometry in which protein synthesis remains conserved as compensation for transcript
94 abundance and architecture divergence across taxa¹⁷. Moreover, specific translational regulation
95 has been extensively observed upon a variety of perturbations to bacteria^{23,24,25,26,27,28,29}. For
96 example, bacteria employ translational quality control and regulation of amino acid biosynthesis
97 in response to amino acid stress³⁰. Thus, translation is a conserved, critical, dynamic, and
98 regulated process in bacteria. However, this level of regulation has thus far been overlooked in
99 mixed bacterial communities. Previous studies of protein synthesis in bacteria have been
100 restricted to pure large-scale cultures (media and RNA inputs up to liters and milligrams,
101 respectively). To date, studying translational regulation in mixed communities or in culture-free
102 contexts has been hindered by low extraction yield, low purity, and the lack of informatic
103 frameworks to study organisms without reference genomes. Consequently, we have a very
104 limited understanding of how widespread bacterial translational regulation may be outside of
105 cultured model organisms.

106 In this work, we develop a method that allows for simultaneous ribosome profiling in a
107 complex community of bacteria without the need for a large-scale, purified cultures. With three
108 lines of evidence, we confirm that MetaRibo-Seq effectively enables translation to be studied in
109 the fecal microbiota. First, the signal consists of footprints that capture the taxonomic diversity
110 of metagenomics, while being locally enriched within coding regions. We identify most
111 enrichment at gene start and stop codons, characteristic of chloramphenicol-treated ribosome
112 profiling³¹. Second, ribosome footprint densities significantly correlate to detectable protein
113 abundances and are significantly enriched in signal for these abundant proteins in these complex
114 bacterial communities. In low diversity human fecal samples, we show that MetaRibo-Seq better
115 correlates with protein abundance and *E. coli* ATP synthase stoichiometry than transcriptomics.
116 Third, biological processes known to be translationally regulated, such as translation itself, are
117 consistently detected as such across multiple samples and taxa. We catalog tens of thousands of
118 genes with evidence of translational regulation in fecal samples across diverse taxa, providing a
119 widespread view of consistent, bacterial translational regulation in these systems. Overall, we
120 show that MetaRibo-Seq facilitates metagenome-wide measurement of bacterial protein
121 synthesis across taxa directly in fecal samples.

122

123 **Results**

124

125 The MetaRibo-Seq workflow.

126

127 MetaRibo-Seq enables sequencing of ribosome-protected footprints directly from human
128 fecal samples (see Methods, Figure 1A). First, we show ribosome profiling can be performed on
129 frozen fecal samples stored in RNAlater^{32, 6} (Ambion), an RNA preserving solution. Unlike
130 some existing protocols^{33,16}, our ribosome profiling protocol first introduces chloramphenicol
131 during lysis. Bead beating lysis is performed to also lyse diverse Gram-positive bacteria³⁴. An
132 ethanol precipitation step post-lysis is introduced to both filter out fecal debris and concentrate
133 RNA and any complexes bound. This has been demonstrated to effectively precipitate
134 ribosomes³⁵. MNase treatment is performed on an extremely crude purification of nucleic acids
135 and complexes. Ribosome profiling performed here uses nearly an order of magnitude less RNA
136 and MNase than isolate protocols typically use (see Methods)^{16, 33}. After high-quality footprints
137 are reliably generated using these methods, ribosome profiling converges to isolate protocols to
138 purify monosomes and prepare libraries³³. MetaRibo-Seq overcome challenges of sample
139 storage, input requirement, bacterial purity, and uniform lysis to generate high quality RNA
140 footprints from fecal samples.

141 Computationally, dealing with short reads and poor or incomplete reference genomes is
142 challenging. To overcome these challenges, we use a *de novo* approach to build references,
143 annotate genes, and map reads to those references (see Methods, Figure 1B). Mapping metrics to
144 *de novo* references are provided (Table S1). We require perfect, unique matches of these
145 ribosome footprints to references to ensure proper mapping. Multi-mapping varies sample to
146 sample, ranging from 6.95 to 26.69 percent. We find that 4.1 - 10.4 percent of mapped reads
147 from RNA technologies performed correspond to predicted coding regions. Given variable
148 amounts of diversity and heterogeneity in any given sample, mapping statistics will vary sample
149 to sample.

150

151 MetaRibo-Seq signal retains taxonomic diversity in human fecal samples.

152

153 MetaRibo-Seq captures taxonomic bacterial diversity in human fecal samples via
154 ribosome-protected footprints. We perform MetaRibo-Seq on four diverse fecal samples. Sample
155 A is from a healthy individual. Sample B is from a patient with a hematological disorder who is
156 undergoing treatment. Sample C is from a patient with a solid malignancy who is undergoing
157 treatment. Sample D is from a patient with Alzheimer’s disease. We also perform MetaRibo-Seq
158 on a low diversity fecal sample from a patient with a hematological disorder who is undergoing
159 antibiotic treatment with metronidazole – Sample E. Metagenomic reads are subjected to *de novo*
160 assembly and gene prediction and annotation for each sample (see Methods). These assemblies
161 and gene predictions are provided (NCBI BioProject #####). Taxonomic differences at the genus
162 level exist between technologies across samples, though most abundant taxa are largely
163 consistent across technologies (Figure 2A). Shannon diversity is also concordant between
164 technologies, including MetaRibo-Seq (Figure 2B). Thus we conclude that MetaRibo-Seq signal
165 faithfully recapitulates the diversity of organisms present in the mixed bacterial communities.
166
167 MetaRibo-Seq signal is characteristic of bacterial ribosome profiling.

168
169 We find that MetaRibo-Seq signal is locally enriched within coding regions. We show
170 average signal across all coding predictions and flanking regions for Samples A, B, C, and D
171 (Figure 3A-D). We visualize strong signal corresponding to predicted ORFs with pronounced
172 signal drop off outside of the start and stop codons for samples A through D (Figure 3A-D).
173 Start and stop codons represent the strongest signal. Surprisingly, MetaRibo-Seq also shows
174 some weak signs of overall codon resolution (Figure S1). In a more targeted analysis, MetaRibo-
175 Seq can achieve stronger codon resolution of ribosomes in common genera. For Sample A and
176 Sample B, assembled contigs of several shared genera are classified and binned appropriately
177 (see Methods). Triplet periodicity is observed across footprint lengths in *Bacteroides* (Figure
178 S2A), *Faecalibacterium* (Figure S2B), and *Alistipes* (Figure S2C). Based purely on raw signal,
179 these findings collectively suggest that MetaRibo-Seq is capturing ribosome-bound footprints as
180 expected.

181
182 MetaRibo-Seq outperforms metatranscriptomics as a proxy for protein abundance in a low
183 diversity fecal sample.

184

185 In Sample E, we identify strong correlations of metatranscriptomics and MetaRibo-Seq to
186 metaproteomics. First, Sample E is dominated by *E. coli*. Interestingly, this *E. coli* is later isolated
187 from the blood of the patient with no single nucleotide variants compared to fecal *E. coli*³⁶. This
188 blood isolate has been sequenced and represents our isolate reference for downstream analyses.
189 In a separate study demonstrating strain identity, this patient is denoted as Patient 3, and Sample
190 E in this study is specifically 27 days prior to bacteremia³⁶. For the 1503 genes that were
191 proteomically-detected in Sample E, we show genus-level representation for
192 metatranscriptomics, MetaRibo-Seq, and metaproteomics (Figure 4A). Of note, 812 of these
193 proteins belong to *E. coli*, while the remaining 691 belong to other taxa. There is greater
194 representation of proteins predicated to arise from *Klebsiella* and *Enterococcus* than transcripts
195 or MetaRibo-Seq signal (Figure 4A). We show a Pearson correlation of 0.46 between MetaRibo-
196 Seq and metaproteomics across the 1503 detected proteins from the metagenomic Sample E
197 (Figure 4B). The Pearson correlation is 0.64 when only considering the 928 detected proteins
198 from the *E. coli* isolate reference (Figure 4C). We display correlations between
199 metatranscriptomics, MetaRibo-Seq, and metaproteomics (Figure 5D). Same technology
200 correlations between the 812 identical protein predictions from the metagenomic and isolate *E.*
201 *coli* analyses all retain Pearson correlations of 0.99. Correlations are weaker in the metagenomic
202 context specifically due to relatively poorer predictions upon addition of the 691 proteins that do
203 not belong to *E. coli*. No previous study to our knowledge provides a correlation between
204 ribosome profiling and proteomics in *E. coli* or any other bacteria; however, this correlation of
205 0.64 is stronger than any cited correlation between transcriptomics and proteomics in isolated,
206 cultured, model *E. coli*³⁷. ATP synthase is a well-characterized complex in terms of
207 stoichiometry in *E. coli* (Figure 4E). We show that MetaRibo-Seq signal better correlates with
208 known ATP synthase stoichiometry than transcriptomics, as expected (Figure 4F-G). Among
209 sequencing technologies, MetaRibo-Seq serves as a better proxy for protein levels and ATP
210 synthase stoichiometry in Sample E *E. coli*.

211

212 MetaRibo-Seq signal significantly correlates to protein abundance and is enriched in these
213 proteins in mixed bacterial communities.

214

215 We find that MetaRibo-Seq significantly correlates to protein abundances as measured by
216 shotgun metaproteomics. In Sample A, we detect 497 proteins. We measure a significant Pearson
217 correlation of 0.32 between MetaRibo-Seq and metaproteomics (Figure 5A). MetaRibo-Seq is
218 better correlated with protein abundance than metatranscriptomics in Sample A (Figure 5B). As
219 expected, both metatranscriptomics and MetaRibo-Seq are significantly enriched in signal for
220 these 497 proteomically-detected genes (Figure 5C). In Sample B, we detect 480 proteins and
221 measure a Pearson correlation of 0.34 between MetaRibo-Seq and metaproteomics (Figure 5D).
222 There is no significant difference in protein abundance prediction between metatranscriptomics
223 and MetaRibo-Seq in Sample B (Figure 5E). Metatranscriptomics and MetaRibo-Seq are
224 similarly enriched in signal for these proteins in Sample B (Figure 5F). These proteins detected
225 by mass spectrometry represent highly abundant bacterial proteins in the fecal samples. These
226 findings suggest that MetaRibo-Seq correlates well with highly abundant protein levels in mixed
227 bacterial communities, and that MetaRibo-Seq signal may thus serve as a surrogate for protein
228 abundance in the study of complex bacterial communities.

229 MetaRibo-Seq signal characteristics and predictive power of protein abundance suggests
230 that it may also prove useful in predicting proteins in taxonomically diverse fecal samples. As a
231 preliminary demonstration of this, we predict small proteins using Prodigal³⁸ with decreased
232 length cutoff (see Methods). We show a histogram of the number of small predictions (20-29
233 amino acids) and the number of those predictions with MetaRibo-Seq RPKM greater than 0.5
234 across samples (Figure S4A). Due to metaproteomic limitations, we are unable to validate these
235 proteins directly. However, we can use a comparative genomic approach to identify clusters of
236 small proteins, all with evidence of translation, that also possess evolutionary signatures
237 indicative of coding regions. We cluster proteins at 70 percent amino acid identity (see
238 Methods). We discover 21 clusters (with at least 4 members) of small proteins across Samples A,
239 B, C, and D that contain both translational evidence among all members in the cluster and
240 significant coding signatures determined via RNACode³⁹ (Figure S3B). We also show greater
241 protein conservation among predictions with MetaRibo-Seq signal than by random chance
242 (Figure S3D). Translational evidence of small proteins in diverse fecal samples decreases the
243 number of predictions to a more conserved subset, suggesting it may be useful in gene
244 prediction.

245

246 Consistent translational regulation is observed across samples and taxa.

247

248 By contrasting metatranscriptomics with MetaRibo-Seq, we identify translationally
249 regulated genes in fecal samples. This provides a widespread view of genes that are consistently
250 translationally regulated within these systems. For Samples A, B, C, and D individually, we
251 show the number of gene predictions and significantly translationally regulated genes (Figure
252 6A). We detect reasonable DESeq2 model fits in comparing between technologies, as shown by
253 the dispersion plots for these analyses for each sample (Figure S4). These significantly
254 translationally regulated genes are clustered at 70 percent amino acid identity for each sample
255 (see Methods, Figure 6B). In a combined analysis (Figure 6C), we define any cluster containing
256 five or more sequences as consistently translationally regulated. The representative sequences for
257 all of these consistently translationally regulated clusters are assigned GO terms with Blast2GO⁴⁰
258 (see Methods). The top 10 most common biological process associated GO terms are displayed,
259 with translation being the top hit (Figure 6D). These sequences and clusters are provided for
260 reference (File S1). Across samples, we catalog 42,267 differentially translated genes and 607
261 consistently translationally regulated gene clusters in these fecal samples, many of which are
262 involved in expected processes, like translation.

263 Other approaches, albeit more biased to known gene annotations, are to rely on Prokka⁴¹
264 annotations. We count the number of times a gene symbol appears as differentially translated
265 (Figure S5) and input those that appear at least five times into a GO Analysis (see Methods,
266 Figure S6). Translation remains the top hit. For Samples A, B, C, and D, we provide GO
267 analysis results of differential genes for each sample individually (Table S2). As a more
268 pathway-oriented analysis, we also determine overrepresentation of pathways among globally
269 differentially translated enzymes based on EC numbers assigned by Prokka⁴¹ (see Methods,
270 Table S3). Amino acid biosynthesis is among the most consistent top hits across samples (Table
271 S3). Thus several approaches lead to expected conclusions of pathways and processes that are
272 translationally regulated.

273

274 **Discussion**

275

276 One of the major limitations in advancing the functional knowledge of microbial
277 communities is an inability to measure the macromolecular output of a given community in an
278 unbiased manner. For example, until now, we have been unable to study fecal bacterial
279 communities, or any *in vivo* system of bacteria, at the level of protein synthesis. Previous
280 approaches have required *in vitro* growth of large, purified cultures; this limits both throughput
281 and the diversity of the sample that can be studied. Here, we introduce a new method, MetaRibo-
282 Seq, and provide evidence that this method enables the human fecal microbiota to be studied at a
283 translational level. In five taxonomically varied samples from human subjects with variable
284 health status, we show MetaRibo-Seq signal retains the taxonomic diversity of the samples. The
285 signal itself is as expected for a chloramphenicol-treated ribosome profiling library – including
286 local enrichment within coding regions and greater enrichment across the start and stop codons
287 of genes. This suggests we have a way to measure bacterial protein synthesis *in vivo* for the first
288 time.

289 To conduct a fair comparison, we perform MetaRibo-Seq on diverse samples but also a
290 lower diversity fecal sample (Sample E) so that more representative protein quantifications of
291 select taxa are achievable. In taxonomically diverse stool samples, MetaRibo-Seq is comparably
292 predictive to protein abundance as metatranscriptomics. However, we show it can be
293 significantly more predictive in a lower diversity scenario. We show that the addition of lower
294 abundant taxa weaken overall correlations in mixed communities. Biologically,
295 metatranscriptomics and MetaRibo-Seq are snapshots of gene transcripts or proteins synthesized,
296 respectively, not direct measurement of the proteins that currently exists. Moreover, significant
297 post-translational differences between taxa likely exist. Technically, it becomes challenging to
298 obtain accurate protein abundances for lowly abundant taxa and proteins in a sample, making
299 such correlations to protein abundance themselves less representative. We conclude that while
300 MetaRibo-Seq can outperform metatranscriptomics within a highly abundant organism, this
301 effect is diminished, perhaps both for biological and technical reasons, when considering all taxa
302 together in diverse communities.

303 There are several limitations to MetaRibo-Seq. First, MetaRibo-Seq does not include
304 steps to degrade RNAs with secondary structure. This is a common issue for ribosome profiling
305 protocols but exacerbated in this *de novo*, low input context^{10, 13}. Though targeted approaches for
306 specific bacteria have been successful for tRNA depletion,²⁶ an untargeted approach, which

307 would be necessary here, has yet to be implemented in literature. Utilization of sucrose density
308 gradients instead of size-exclusion chromatography columns may also prove valuable in
309 removing various structured RNAs; however, downstream ribosome profiling input requirements
310 likely make this challenging to address. This limitation may, however, enable other types of
311 investigation; for example, signal corresponding to structured RNAs will likely be useful to
312 predict novel structured RNAs in non-coding regions. Experimental modifications will also
313 likely improve these limitations.

314 We anticipate that MetaRibo-Seq will enable a clearer functional view of the fecal
315 microbiota. With increasing use of metatranscriptomics, we envision that MetaRibo-Seq will be
316 applied to various disease states to better probe the microbiota and its functions. We especially
317 anticipate MetaRibo-Seq will be used longitudinally to study translational regulation of
318 genomically-stable, clinically-relevant taxa. MetaRibo-Seq signal provides unique features like
319 enrichment within coding regions, greater enrichment at the start and end of genes, and, as we
320 show, some signs of codon-level resolution in some taxa. Future work will likely include using
321 these features for gene prediction, which is particularly challenging when studying metagenomic
322 samples and small proteins⁴². To validate such predictions, significant methods development and
323 improvements in metaproteomics will be needed. With direct proteomic evidence often
324 unattainable, coding potential, translational evidence, and conservation among predictions
325 present themselves as the strongest lines of evidence proteins, especially small proteins, exists in
326 the fecal microbiota (Figure S6 and File S2). We also expect MetaRibo-Seq to be applied to
327 other culture-free conditions, perhaps requiring other modifications. Overall, we show that
328 translation can be comprehensively studied in mixed bacterial communities in a culture-free
329 manner. This method also sheds light on consistently translationally regulated genes *in vivo* in a
330 comprehensive, metagenome-wide analysis.

331

332 **Materials and Methods**

333

334 **Subject Recruitment**

335 MetaRibo-Seq was performed on fecal samples from individuals from a variety of health
336 states. Informed consent was obtained for all participants. None of the participants received
337 bacterial translation inhibitors. All subjects were recruited at Stanford University as a part of one

338 of three IRB-approved protocols for tissue biobanking and clinical metadata collection (PIs: Dr.
339 Ami Bhatt, Dr. Victor Henderson, Dr. David Miklos).

340

341 **Fecal Samples Storage**

342 Stool was immediately stored in 2 mL cryovials and frozen at -80 °C. Stool was not
343 thawed until lysis. For RNA extraction applications, 1.3 grams of fecal samples were preserved
344 in 700 µL of RNALater (Ambion) at -80 °C.

345

346 **Cell Lysis for Metatranscriptomics and MetaRibo-Seq**

347 Stool (150 mg) was suspended in 600 µL Qiagen RLT lysis buffer supplemented with
348 one percent beta-mercaptoethanol and 0.3 U/µL Superase-In (Invitrogen). For MetaRibo-Seq
349 lysis, 1.55 mM of chloramphenicol was also added to this lysis solution, and the solution was
350 incubated at room temperature for 5 minutes. The suspension was subjected to bead beating for 3
351 minutes using 1.0 mm Zirconia/Silica beads. This was performed with a MiniBeadBeater-16,
352 Model 607. The lysed solution was centrifuged at room temperature for 3 minutes at 21,000 x g
353 to pellet cellular debris, and the supernatant was extracted to 2 mL tubes.

354

355 **Metagenomics**

356 DNA was extracted from fecal samples with DNA Stool Mini Kit (Qiagen) using
357 manufacture protocols. Samples were exposed to bead beating for 3 minutes. 1 ng of DNA was
358 used to create Nextera XT libraries according to manufacturer's instructions (Illumina).

359

360 **MetaRibo-Seq**

361 The lysis supernatant was subjected to ethanol precipitation with 0.1 percent volume 3M
362 sodium acetate and 2.5 volumes of 100 percent ethanol. To precipitate, samples were incubated
363 at -80 °C for 30 minutes, then centrifuged at 21,000 x g for 30 minutes at 4 °C. This was a rough
364 purification specifically implemented to enable suspension of concentrated RNA from
365 reasonable input of fecal sample. The pellet of RNA and RNA-protein complexes was
366 resuspended in MNase buffer. The buffer contained 25 mM Tris pH 8.0, 25 mM NH₄Cl, 10 mM
367 MgOAc, and 1.55 mM chloramphenicol. To resuspend, we quickly broke the pellet apart with a
368 pipette tip and vortexed for 15 seconds. 1 µL of solution was diluted 20 fold and quantified with

369 Qubit dsDNA HS Assay Kit (Invitrogen). MNase reaction mix was prepared as described³³,
370 except this was scaled down to an input of 80 µg of RNA and 1 µL of NEB MNase 500 U/µL in
371 a total reaction volume of 200 µL. The MNase reaction was incubated at room temperature for 2
372 hours. All following steps were performed identically³³, except the tRNA removal steps were
373 excluded. Briefly, 500 µL of polysome binding buffer was used to wash the Sephacryl S400
374 MicroSpin columns (GE Healthcare Life Sciences) three times - spinning the column for 3
375 minutes at 4 °C at 600 RPM. Polysome binding buffer consisted of 100 µL Igepal CA-630, 500
376 µL magnesium chloride at 1M, 500 µL EGTA at 0.5 M, 500 µL of NaCl at 5M, 500 µL Tris-HCl
377 pH 8.0. at 1M, and 7.9 mL of RNase-free water. The MNase reaction was applied to the column
378 and centrifuged for 5 minutes at 4 °C. The flow through was purified further with miRNAeasy
379 Mini Kit (Qiagen) using manufacture protocols. Elution was performed at 15 µL volume. rRNA
380 was depleted using RiboZero-rRNA Removal Kit for Bacteria (Illumina) using manufacture
381 protocol, except all reaction volumes and amounts were reduced by 50 percent. This was purified
382 with RNAeasy MinElute Cleanup Kit (Qiagen), eluting in 20 µL. The reaction, in 18 µL volume
383 at a total of 100 ng, was subjected to T4 PNK Reaction (NEB M0201S) with addition of 1µL
384 Superase-In (Invitrogen), 2.2 µL 10X T4 PNK Buffer, and 1 µL T4 PNK (10U/µL). This
385 reaction was purified again with RNAeasy MinElute Cleanup (Qiagen). The concentration was
386 determined with Qubit RNA HS Assay Kit (Illumina). With 100 ng as input, libraries were
387 prepared using NEBNext Small RNA Library Prep Set for Illumina (NEB, E7330), using
388 manufacture protocols. DNA was purified using Minelute PCR Purification Kit (Qiagen).

389

390 **Small Metatranscriptomics of Fecal Samples**

391 We performed metatranscriptomics as follows: 15 µL of proteinase K (Ambion, 20
392 mg/mL) was added to 600 µL of lysate. After incubation for 10 minutes at room temperature,
393 samples were centrifuged at 21,000 x g for 3 minutes and the supernatant was collected. An
394 equal volume of Phenol/Chloroform/Isoamyl Alcohol 25:24:1 (pH. 5.2) was applied and vortex
395 for three minutes. The mixture was centrifuged at 21,000 x g for three minutes. The aqueous
396 phase was extracted. This was repeated once more. The final aqueous phase was ethanol
397 precipitated. The RNA was further purified using the RNAeasy Mini plus Kit (Qiagen) using
398 manufacture protocols. Any remaining DNA was degraded via Baseline-ZERO-Dnase
399 (Epicentre) using manufacture protocols. RNA was fragmented for 15 minutes at 70 °C using

400 RNA Fragmentation Reagent (Ambion) using manufacture protocols. At this point, the
401 MetaRibo-Seq and small metatranscriptomics protocol completely converge. The fragmented
402 RNA was purified with miRNAeasy Mini Kit (Qiagen) using manufacture protocols. Elution was
403 performed at 15 μ L. rRNA was depleted using RiboZero-rRNA Removal Kit for Bacteria
404 (Illumina) using half reactions of manufacture protocol. This was purified with RNAeasy
405 MinElute Cleanup Kit (Qiagen), eluting in 20 μ L. The fragments, in 18 μ L volume, were
406 subjected to T4 PNK Reaction (NEB M0201S) with addition of 1 μ L Superase-In (Invitrogen),
407 2.2 μ L 10X T4 PNK Buffer, and 1 μ L T4 PNK (10U/ μ L). This reaction was purified again with
408 RNAeasy MinElute Cleanup (Qiagen). The concentration was determined with Qubit RNA HS
409 Assay Kit (Invitrogen). With 100 ng as input, libraries were prepared using NEBNext Small
410 RNA Library Prep Set for Illumina (NEB, E7330), using manufacture protocols. DNA was
411 purified using MinElute PCR Purification Kit (Qiagen).

412

413 **Differential Centrifugation and FASP for Metaproteomics**

414 To remove human proteins, fecal samples were subjected to differential centrifugation.
415 100 mg of fecal sample was suspended in 1x PBS in 1.7 mL Eppendorf tubes. The tubes were
416 centrifuged at 600 x g for 1 minute at room temperature. The supernatant was collected in a clean
417 Eppendorf tube and centrifuged at 10,000 x g for 1 minute at room temperature. The supernatant
418 was decanted and the pellet was resuspended in 1 mL of PBS. The process was repeated once
419 more. The final pellet was resuspended in 2% SDS, 100 mM DTT, and 20 mM Tris HCl, pH 8.8
420 with protease inhibitor. These cells were subjected to bead beating for 3 minutes with a
421 MiniBeadBeater-16, Model 607. 1mM zirconia/silica beads were used. Tubes were centrifuged
422 for 3 minutes and clarified lysate in the supernatant was collected. Lysate was prepared using
423 FASP⁴³ with the same minor modifications previously documented⁴⁴. Every step involved a
424 centrifugation step for 15 minutes at 14,000 x g. Samples were diluted tenfold in 8 M urea and
425 loaded into Microcon Ultracel YM-30 filtration devices (Millipore). They were washed in 8 M
426 urea, reduced for 30 minutes in 10 mM DTT, and alkylated in 50 mM iodoacetamide for 20
427 minutes. Samples were washed three times in 8M urea and two times in 50 mM ammonium
428 bicarbonate. Trypsin (Pierce 90057) (1:100 enzyme-to-protein ratio) was added and incubated
429 overnight at 37 °C. Into a new collection tube, samples were centrifuged and further eluted in 50
430 μ L of 70 percent acetonitrile and 1 percent formic acid. The mixture was brought to dryness for

431 one hour using a Savant SPD121P SpeedVac concentration at 30°C, then resuspended in 0.2
432 percent formic acid⁴⁴.

433

434 **Metaproteomics**

435 LC-MS/MS analysis was performed by the Stanford University Mass Spectrometry
436 Facility using the Thermo Orbitrap Fusion Tribrid. A Thermo Scientific Orbitrap Fusion coupled
437 to a nanoAcquity UPLC system (Waters, M Class) was used to collect mass spectra (MS).
438 Samples were loaded on a 25 cm sub 100 micron C18 reverse phase column packed in-house
439 with a 80 minute gradient at a flow rate of 0.45 µL/min. The mobile phase consisted of: A (water
440 containing 0.2% formic acid) and B (acetonitrile containing 0.2% formic acid). A linear gradient
441 elution program was used: 0–45 min, 6–20 % (B); 45-60 min, 35 % (B); 60-70 min, 45 % (B);
442 70-71 min, 70 % (B); 71-77 min, 95 % (B); 77-80 min, 2 % (B). Ions were generated using
443 electrospray ionization in positive mode at 1.6 kV. MS/MS spectra were obtained using Collision
444 Induced Fragmentation (CID) at a setting of 35 of arbitrary energy. Ions were selected for
445 MS/MS in a data dependent, top 15 format with a 30 second exclusion time. Scan range was set
446 to 400 – 1500 m/z. Typical orbitrap mass accuracy was below 2 ppm; for analysis. A 12 ppm
447 window was allowed for precursor ions and 0.4 Da for the fragment ions for CID fragmentation
448 detected in the ion trap. Prokka-predicted⁴¹ proteins were used as a reference database for protein
449 detection using the Byonic proteomics search pipeline v 2.10.5⁴⁵. Byonic parameters include:
450 spectrum-level FDR auto, digest cutter C-terminal cutter, peptide termini semi-specific,
451 maximum number of missed cleavages 2, fragmentation type CID low energy, precursor
452 tolerance 12.0 ppm, fragment tolerance 0.4 ppm, protein FDR cutoff 1 percent. These methods
453 were performed by Stanford Mass Spectrometry Facility (SUMS). Using spectral count output,
454 Normalized Spectral Abundance Factor (NSAF) was calculated by in house scripts.

455

456 **De Novo Assembly**

457 Quality trimmed metagenomic reads were assembled using metaSPAdes 3.7.0⁴⁷. For all
458 samples, a maximum of 60 million metagenomic reads was used to generate assemblies. Samples
459 sequenced to higher depth were randomly subsetted to 60 million for assembly purposes to both
460 ensure relatively similar numbers of gene predictions and limit computational requirements in
461 assembly and downstream predictions.

462

463 **Read Mapping, Gene Prediction and Annotation**

464 Reads were trimmed with trim galore version 0.4.0 using cutadapt 1.8.1⁴⁶ with flags `-q`
465 `30` and `-illumina`. Reads were mapped to the annotated assembly using bowtie version 1.1.1⁴⁸.
466 To avoid all possible conservation conflicts in downstream differential analysis, only perfect,
467 unique short read alignments were considered. IGV⁴⁹ was used to visualize coverage. Prokka
468 v1.12⁴¹ was used to predict genes from the metagenomics assemblies using the `-meta` option.
469 Annotations were facilitated by many dependencies^{38,50,51,52}. For small protein predictions,
470 prodigal³⁸ was performed after lowering the size threshold from 90 bases to 60 bases.

471

472 **Read density as a function of position**

473 MetaRibo-seq reads were mapped to their metagenomic assemblies. The assembly and
474 aligned reads were analyzed with RiboSeqR⁵³. CDSs (coding sequences) were predicted using
475 the findCDS function. Ribosome profiling counts for predicted CDSs were determined with the
476 sliceCounts function. CDSs were filtered to contain at least 10 reads.

477

478 **Taxonomic Classification of Technologies**

479 Reads mapping specifically to Prokka-predicted⁴¹ coding regions were counted. That
480 entire genomic element was input into One Codex⁵⁴ for classification equal to the number of
481 reads mapping to it. This enabled fair comparisons between technologies, as the small
482 metatranscriptomics and MetaRibo-Seq reads can be too small to classify individually with *k*-
483 mer-based approaches. Though metagenomic reads were long enough to be classified directly,
484 they were also subject to the same analysis – entire genes are classified in equal number to the
485 reads overlapping them. Thus, all taxonomy plots represent entire gene classifications and are
486 dependent on the assembly.

487

488 **Differential Analysis**

489 The number of reads mapping to a given region were calculated with bedtools multicov⁵⁹.
490 Strandedness was enforced for metatranscriptomics and MetaRibo-Seq. All differential analyses
491 were performed using these counts with all conditions performed in duplicate via DESeq2⁶⁰. A
492 gene was considered differential if it had log2fold change above 1 or below -1, while also

493 reaching an FDR < 0.05. Results were displayed as volcano plots or tables. Heatmaps were
494 created using gplots⁶¹. Reads per Kilobase Million (RPKM) calculations were performed using
495 in house scripts.

496

497 **Statistical Analysis**

498 All Pearson correlations were calculated in R using the Hmisc package⁵⁵. Scatterplots
499 were created with ggplot2⁵⁶. Significance between Pearson correlations was assigned via cocor⁵⁷.
500 Significant differences between RPKM values were assigned using the Kruskal-Wallis test.
501 Significance was assigned as * p value < 0.05, *** p value < 0.001. Zou's⁵⁸ 95 percent
502 confidence intervals were assigned *** if there is no overlap with 0 in the interval.

503

504 **Protein Clustering Analysis**

505 For analyses independent of gene annotation, significantly translationally regulated
506 proteins were clustered using Cd-hit⁶² with 70 percent amino acid identity. Representative
507 sequences were input into Blast2GO⁴⁰ using the nr database. Small protein predictions with
508 translational evidence were also clustered using this same approach. Coding potential was
509 assessed using RNAcode³⁹ using the p value assigned to the predicted reading frame.

510

511 **Triplet Periodicity Analysis**

512 Using the same default parameters as read density as a function of position, triplet
513 periodicity was called using RiboSeqR⁵³. To analyze triplet periodicity of specific genera,
514 assembled contigs were classified using One Codex⁵⁴. Contigs that classified into a specific
515 genus were binned together. Only reads mapping specifically to these bins were considered.

516

517 **GO Analysis**

518 Based on differential genes from DESeq2⁶⁰ analyses, UniProt⁶³ genes annotated by
519 Prokka⁴¹ were input into David Functional Annotation^{64,65}. All species detected were used as
520 background for these metagenomic analyses.

521

522 **Pathway Analysis**

523 Prokka⁴¹ predicted genes with associated EC (enzyme) numbers were considered. For a
524 given sample, all the reads mapping to any gene with a specific EC number were summed for
525 metatranscriptomics and MetaRibo-Seq. DESeq2⁶⁰ called differential enzymes using
526 MicrobiomeAnalyst⁶⁶. Network mapping is performed to identify pathways corresponding to
527 differential enzymes.

528

529 **Acknowledgements**

530 The authors would like to thank Tessa M Andermann, Ekaterina Tkachenko, and Joyce
531 B. Kang for major contributions to the fecal biobank of bone marrow transplant patients at
532 Stanford hospital. We would like to thank the patients and nurses involved in collection. We
533 thank Christina Wyss-Coray for collecting Alzheimer's samples used in this study. We
534 appreciate sample collection feedback from Victor Henderson and Tony Wyss-Coray. We thank
535 Anshul Kundaje and Georgi Marinov for helpful computational analysis guidance. We would
536 also like to thank Stanford University Mass Spectrometry for performing and analyzing mass
537 spectrometry on the FASP fecal samples. Sequencing costs were supported via NIH S10 Shared
538 Instrumentation Grant (1S10OD02014101) and Damon Runyon Clinical Investigator Award to
539 ASB, Stanford ADRC grant # P50AG047366. B.J.F is supported by National Science
540 Foundation Graduate Research Fellowship DGE-114747.

541

542 **Figure Legends**

543

544 **Figure 1**

545 Workflow of ribosome profiling.

546 (A) Experimental workflow of MetaRibo-Seq. Chloramphenicol halts translation, the bacterial
547 community is lysed, MNase is used to create footprints, and footprints are converted to
548 sequencing libraries.

549 (B) Computational workflow of the multi-omics approach. *De novo* assemblies are created and
550 annotated, predicted genes are quantified at multi-omic levels, and taxonomy, correlations, and
551 differential abundance are determined from these results.

552

553 **Figure 2**

554 MetaRibo-Seq signal captures diversity in a metagenomic context.

555 (A) Genus-level classifications of all sequencing technologies performed on Samples A, B, C, D,
556 and E. Replicates for metatranscriptomics and MetaRibo-Seq are shown for reproducibility. Taxa
557 represented below three percent are grouped into “Other” for visual purposes.

558 (B) Shannon diversities across technologies for these samples are displayed.

559

560 **Figure 3**

561 MetaRibo-Seq signal is characteristic of chloramphenicol-treated ribosome profiling in bacteria
562 across diverse samples.

563 (A-D) Average MetaRibo-Seq signal across genes and flanking regions for Sample A, B, C, and
564 D, respectively. Every predicted open reading frame containing at least 10 reads are included in
565 the analysis.

566

567 **Figure 4**

568 In a low diversity fecal sample, MetaRibo-Seq is a significantly better predictor than
569 metatranscriptomics of protein abundance and ATP synthase stoichiometry in *E. coli*.

570 (A) In Sample E, there are 1503 proteomically-detectable genes. Only focusing on these genes,
571 we taxonomically classify the entire gene in equal number to the reads (for metatranscriptomics
572 and MetaRibo-Seq) or spectral counts (for metaproteomics) assigned to it (see Methods).

573 (B) Scatterplot of MetaRibo-Seq RPKM and metaproteomics NSAF log-scaled for these 1503
574 genes.

575 (C) Scatterplot of MetaRibo-Seq RPKM and metaproteomics NSAF log-scaled only for the 928
576 proteomically-detected genes predicted from isolate *E. coli*.

577 (D) Pearson correlations for pairwise comparisons across technologies. Blue bars indicate
578 Pearson correlations pertaining to the entire metagenomic Sample E. The correlations between
579 metatranscriptomics vs. MetaRibo-Seq, metatranscriptomics vs. metaproteomics, and MetaRibo-
580 Seq vs. metaproteomics are 0.85, 0.39, and 0.46, respectively. All are significant (p value $< 2^{-16}$).
581 MetaRibo-Seq is a significantly better predictor of protein levels with Zou’s⁵⁸ 95 % confidence
582 interval between -0.0917 to -0.0487. Red bars indicate Pearson correlations pertaining to the
583 isolated *E. coli* in the sample. The correlations between metatranscriptomics vs. MetaRibo-Seq,
584 metatranscriptomics vs. metaproteomics, and MetaRibo-Seq vs. metaproteomics are 0.90, 0.53,

585 and 0.64, respectively. All are significant (p value $< 2^{-16}$). MetaRibo-Seq is a significantly better
586 predictor of protein levels with Zou's⁵⁸ 95 % confidence interval between -0.1352 to -0.0868.

587 (E) F0F1 ATP synthase in *E. coli* forms with a specific stoichiometry as visualized.

588 (F) Correlation between log-scaled metatranscriptomics RPKM and expected ATP synthase
589 stoichiometry in complex. The Pearson correlation is 0.56 (p value = 0.1475)

590 (G) Correlation between log-scaled MetaRibo-Seq RPKM and expected ATP synthase
591 stoichiometry in complex. The Pearson correlation is 0.92 (p value = 0.0012).

592

593 **Figure 5**

594 MetaRibo-Seq signal significantly correlates to metaproteomics and is enriched for these
595 products

596 (A) For Sample A, scatterplot of MetaRibo-Seq RPKM (Reads per Kilobase Million) and
597 metaproteomics NSAF (Normalized Spectral Abundance Factor) both log10-scaled. 497 genes
598 are displayed.

599 (B) Pairwise Pearson correlations between log-scaled metatranscriptomics RPKM, MetaRibo-
600 Seq RPKM, and metaproteomics NSAF for these 497 genes. Pearson correlations are 0.88, 0.26,
601 and 0.32 for metatranscriptomics vs. MetaRibo-Seq, metatranscriptomics vs. metaproteomics,
602 and MetaRibo-Seq vs. metaproteomics, respectively. All are significant (p value $< 2^{-16}$).

603 MetaRibo-Seq is a significantly better predictor of protein levels than metatranscriptomics for
604 these proteins in Sample A with a Zou's⁵⁸ 95 % confidence interval between -0.1322 and -
605 0.0480.

606 (C) Metatranscriptomics and MetaRibo-Seq RPKM for all predicted genes compared to those
607 detected by metaproteomics. Both metatranscriptomic and MetaRibo-Seq signal for
608 proteomically-detected proteins are significantly enriched (p value $< 2^{-16}$).

609 (D) For Sample B, scatterplot of MetaRibo-Seq RPKM and metaproteomics NSAF both log10-
610 scaled. 497 genes are displayed.

611 (E) Pairwise Pearson correlations between log-scaled metatranscriptomics RPKM, MetaRibo-
612 Seq RPKM, and metaproteomics NSAF for these 480 genes. Pearson correlations are 0.89, 0.36,
613 and 0.34 for metatranscriptomics vs. MetaRibo-Seq, metatranscriptomics vs. metaproteomics,
614 and MetaRibo-Seq vs. metaproteomics, respectively. All are significant (p value $< 2^{-16}$).

615 (F) Metatranscriptomics and MetaRibo-Seq RPKM for all predicted genes compared to those
616 detected by metaproteomics. Both metatranscriptomic and MetaRibo-Seq signal for
617 proteomically-detected proteins are significantly enriched (p value $< 2^{-16}$).

618

619 **Figure 6**

620 Genes that are consistently translationally regulated emerged across samples and taxa.

621 (A) For Samples, A, B, C, and D, we show the number of total gene predictions via Prokka⁴¹. We
622 performed DESeq2⁶⁰ on these individually, comparing metatranscriptomics to MetaRibo-Seq.

623 We show the number of those genes identified as translationally (absolute value(log₂ fold
624 change) > 1 and FDR < 0.05). We predict 223630, 196683, 272895, and 173624 genes from
625 Sample A, B, C, and D, respectively. Among these, 11872, 6580, 15188, and 8647, respectively,
626 are called significant translationally regulated genes.

627 (B) Significant translationally regulated genes are converted to proteins and clustered at 70
628 percent amino acid identity (see Methods). The number of clusters with specific numbers of
629 sequences are displayed, jittered and color-coded for each sample.

630 (C) The number of clusters with specific numbers of sequences combined across Samples A, B,
631 C, and D

632 (D) If the combined cluster contained at least 5 sequences, this gene is considered consistently
633 translationally regulated. 607 clusters met this requirement. For these clusters, the representative
634 sequence (see Methods) is selected to represent the entire cluster. These representatives were
635 input into Blast2GO to assign GO terms based on protein sequence.

636

637 **Figure S1**

638 MetaRibo-Seq demonstrates some weak signs of overall codon-resolution.

639 (A-D) Triplet periodicity across footprint lengths for Sample A, B, C, and D, respectively.

640 Colors indicate which frame a read falls within.

641

642 **Figure S2**

643 MetaRibo-Seq demonstrates stronger codon resolution in taxa-specific analyses.

644 (A) All contigs assigned to the genera Bacteroides are considered from Sample A and B,
645 respectively. Only these contigs are considered in triplet periodicity analyses.

646 (B and C) The same triplet periodicity analysis for Faecalibacterium and Alistipes, respectively.

647

648 **Figure S3**

649 Small protein predictions with translational evidence demonstrate strong conservation.

650 (A) Breakdown of small protein predictions across Samples A, B, C, and D, and those with
651 translational evidence (MetaRibo-Seq signal above 0.5 RPKM).

652 (B) Genus-level classification of small protein predictions across Samples A, B, C, and D.

653 Relative proportions of small proteins including all predictions and only those with translational
654 evidence are provided.

655 (C) The 6,774 small proteins with translational evidence are clustered at 70 percent amino acid
656 identity. 47 clusters with at least 4 members are identified. Among these, 21 clusters possess
657 evolutionary signatures indicative of coding regions (p values < 0.001) via RNACode³⁹.

658 (D) In dark red, clustering with 70 percent protein identity of small proteins with translational
659 evidence – 6,774 proteins across all samples. In orange, clustering with 70 percent amino acid
660 identity of 6,744 small proteins randomly chosen from prodigal predictions; an equal number of
661 proteins as those with translational evidence from each sample were randomly chosen.

662

663 **Figure S4**

664 DESeq2 models adequately fit dispersion in comparing metatranscriptomics to MetaRibo-Seq.

665 (A-D) Dispersion plots of DESeq2 models fit to Samples A, B, C, and D, respectively.

666

667 **Figure S5**

668 Numerous genes are consistently translationally regulated in the fecal microbiota

669 (A) For Samples A, B, C and D, we show genera level classifications of translationally regulated
670 genes assigned UniProt³¹ protein IDs.

671 (B-E) Volcano plots comparing metatranscriptomics and MetaRibo-Seq in Sample A, B, C, and
672 D, respectively. Significant genes are colored in red. The four most consistently translationally
673 regulated genes are also denoted.

674

675 **Figure S6**

676 In depth analysis of consistently translationally regulated genes with assigned names in the fecal
677 microbiota across Samples A, B, C, and D.

678 (A) Top 40 most common translationally regulated genes across samples. Heatmap intensity
679 represents the number of times the gene appeared differential in a sample.

680 (B) GO analysis including genes that are differentially translated at least 5 times across samples.

681

682 **Table S1**

683 Mapping statistics to *de novo* references. This table shows the number of reads, percentage of
684 reads mapping to the assembly, and percentage of reads overlapping regions annotated as coding.

685

686 **Table S2**

687 GO analysis of significant translationally regulated genes for Samples A, B, C, and D. Only
688 genes assigned UniProt⁶³ protein IDs are considered. Significant IDs are called with DESeq2⁶⁰.
689 These are input into David⁶⁴.

690

691 **Table S3**

692 Pairwise comparison of metatranscriptomics to MetaRibo-Seq across Sample A, B, C, and D.
693 Only predicted genes with EC numbers are considered. Significant differences in EC numbers
694 are called with DESeq2⁶⁰. Negative log₂FC means lower in the technology first listed in the tab
695 under consideration. EC numbers and their associated adjusted p value are input into
696 MicrobiomeAnalyst⁶⁶ to determine overrepresented pathways based on differential EC numbers.

697

698 **Table S4**

699 We display all correlations between replicates and technologies for Samples A, B, C, and D. For
700 each sample, we provide correlations between metatranscriptomics replicates, MetaRibo-Seq
701 replicates, metagenomics versus metatranscriptomics, metagenomics versus MetaRibo-Seq,
702 metatranscriptomics versus MetaRibo-Seq, and metagenomics versus translation efficiency (TE
703 – ratio of MetaRibo-Seq and metatranscriptomics).

704

705 **File S1**

706 We provide sequences for every protein in Samples A, B, C, and D that are translationally
707 regulated in the gut microbiota. Translationally regulated proteins (.faa) and 70 percent identity
708 clustering (.clstr) are provided for Samples A, B, C, and D. The representative sequences for
709 clusters (.faa) with more than 5 sequences for samples are also provided. The sequence name
710 itself denotes which sample the sequence is found in. Any sequence that begins with a specific
711 identifier can be linked to a sample: HDALDHFB = Sample A, HENMDNCI =Sample B,
712 PJJNKMKO = Sample C, GPBGMPE = Sample D. Blast2GO⁴⁰ results for the representative
713 sequences of consistent clusters are provided.

714

715 **File S2**

716 We contribute sequences of small proteins we identified. Small protein predictions using
717 prodigal³⁸ with lower size threshold (60 bp) for Samples A, B, C, and D individually (.faa) are
718 provided. Small protein predictions with MetaRibo-Seq RPKM above 0.5 for the four samples
719 individually (.faa) are given. Combined clustering of these small proteins with translational
720 evidence are provided (.clstr). Those translated clusters with more than 3 sequences and with
721 RNACode p values < 0.001 are provided in the “smallproteinsequences” folder named by the
722 cluster they belong to.

723

724 **Bibliography**

725

- 726 1. Klassen, J. L. Defining microbiome function. *Nat. Microbiol.* **3**, 864–869 (2018).
- 727 2. Petriz, B. A. & Franco, O. L. Metaproteomics as a Complementary Approach to Gut
728 Microbiota in Health and Disease. *Front. Chem.* **5**, 4 (2017).
- 729 3. Wilmes, P., Heintz-Buschart, A. & Bond, P. L. A decade of metaproteomics: Where we
730 stand and what the future holds. *Proteomics* **15**, 3409–3417 (2015).
- 731 4. Lichtman, J. S., Sonnenburg, J. L. & Elias, J. E. Monitoring host responses to the gut
732 microbiota. *ISME J.* **9**, 1908–1915 (2015).

- 733 5. Hyatt, D., LoCascio, P. F., Hauser, L. J. & Uberbacher, E. C. Gene and translation initiation
734 site prediction in metagenomic sequences. *Bioinforma. Oxf. Engl.* **28**, 2223–2230 (2012).
- 735 6. Franzosa, E. A. *et al.* Relating the metatranscriptome and metagenome of the human gut.
736 *Proc. Natl. Acad. Sci.* **111**, E2329–E2338 (2014).
- 737 7. Mehta, R. S. *et al.* Stability of the human faecal microbiome in a cohort of adult men. *Nat.*
738 *Microbiol.* **3**, 347–355 (2018).
- 739 8. Schirmer, M. *et al.* Dynamics of metatranscription in the inflammatory bowel disease gut
740 microbiome. *Nat. Microbiol.* **3**, 337–346 (2018).
- 741 9. Metatranscriptome of human faecal microbial communities in a cohort of adult men | Nature
742 Microbiology. Available at: <https://www.nature.com/articles/s41564-017-0084-4>. (Accessed:
743 17th April 2018)
- 744 10. Ingolia, N. T., Ghaemmaghami, S., Newman, J. R. S. & Weissman, J. S. Genome-wide
745 analysis in vivo of translation with nucleotide resolution using ribosome profiling. *Science*
746 **324**, 218–223 (2009).
- 747 11. Ingolia, N. T. Ribosome Footprint Profiling of Translation throughout the Genome. *Cell* **165**,
748 22–33 (2016).
- 749 12. Cenik, C. *et al.* Integrative analysis of RNA, translation, and protein levels reveals distinct
750 regulatory variation across humans. *Genome Res.* **25**, 1610–1621 (2015).
- 751 13. Li, G.-W., Burkhardt, D., Gross, C. & Weissman, J. S. Quantifying absolute protein
752 synthesis rates reveals principles underlying allocation of cellular resources. *Cell* **157**, 624–
753 635 (2014).

- 754 14. Mohammad, F., Woolstenhulme, C. J., Green, R. & Buskirk, A. R. Clarifying the
755 Translational Pausing Landscape in Bacteria by Ribosome Profiling. *Cell Rep.* **14**, 686–694
756 (2016).
- 757 15. Li, G.-W., Oh, E. & Weissman, J. S. The anti-Shine-Dalgarno sequence drives translational
758 pausing and codon choice in bacteria. *Nature* **484**, 538–541 (2012).
- 759 16. Woolstenhulme, C. J., Guydosh, N. R., Green, R. & Buskirk, A. R. High-Precision Analysis
760 of Translational Pausing by Ribosome Profiling in Bacteria Lacking EFP. *Cell Rep.* **11**, 13–
761 21 (2015).
- 762 17. Lalanne, J.-B. *et al.* Evolutionary Convergence of Pathway-Specific Enzyme Expression
763 Stoichiometry. *Cell* **173**, 749-761.e38 (2018).
- 764 18. Meyer, M. M. The role of mRNA structure in bacterial translational regulation. *Wiley*
765 *Interdiscip. Rev. RNA* **8**, (2017).
- 766 19. Zengel, J. M. & Lindahl, L. Diverse Mechanisms for Regulating Ribosomal Protein
767 Synthesis in Escherichia coli. in *Progress in Nucleic Acid Research and Molecular Biology*
768 (eds. Cohn, W. E. & Moldave, K.) **47**, 331–370 (Academic Press, 1994).
- 769 20. Lindahl, L., Jaskunas, S. R., Dennis, P. P. & Nomura, M. Cluster of genes in Escherichia coli
770 for ribosomal proteins, ribosomal RNA, and RNA polymerase subunits. *Proc. Natl. Acad.*
771 *Sci.* **72**, 2743–2747 (1975).
- 772 21. Fallon, A. M., Jinks, C. S., Strycharz, G. D. & Nomura, M. Regulation of ribosomal protein
773 synthesis in Escherichia coli by selective mRNA inactivation. *Proc. Natl. Acad. Sci.* **76**,
774 3411–3415 (1979).
- 775 22. Dean, D. & Nomura, M. Feedback regulation of ribosomal protein gene expression in
776 Escherichia coli. *Proc. Natl. Acad. Sci.* **77**, 3590–3594 (1980).

- 777 23. Bucca, G. *et al.* Translational control plays an important role in the adaptive heat-shock
778 response of *Streptomyces coelicolor*. *Nucleic Acids Res.* **46**, 5692–5703 (2018).
- 779 24. Sawyer, E. B., Grabowska, A. D. & Cortes, T. Translational regulation in mycobacteria and
780 its implications for pathogenicity. *Nucleic Acids Res.* doi:10.1093/nar/gky574
- 781 25. C. Taylor, R. *et al.* Changes in translational efficiency is a dominant regulatory mechanism
782 in the environmental response of bacteria. *Integr. Biol.* **5**, 1393–1406 (2013).
- 783 26. Morita, Y., Gilmour, C., Metcalf, D. & Poole, K. Translational Control of the Antibiotic
784 Inducibility of the PA5471 Gene Required for mexXY Multidrug Efflux Gene Expression in
785 *Pseudomonas aeruginosa*. *J. Bacteriol.* **191**, 4966–4975 (2009).
- 786 27. Starosta, A. L., Lassak, J., Jung, K. & Wilson, D. N. The bacterial translation stress response.
787 *FEMS Microbiol. Rev.* **38**, 1172–1201 (2014).
- 788 28. Jeong, Y. *et al.* The dynamic transcriptional and translational landscape of the model
789 antibiotic producer *Streptomyces coelicolor* A3(2). *Nat. Commun.* **7**, 11605 (2016).
- 790 29. Mathieu, A. *et al.* Discovery and Function of a General Core Hormetic Stress Response in *E.*
791 *coli* Induced by Sublethal Concentrations of Antibiotics. *Cell Rep.* **17**, 46–57 (2016).
- 792 30. Bullwinkle, T. J. & Ibba, M. Translation quality control is critical for bacterial responses to
793 amino acid stress. *Proc. Natl. Acad. Sci.* **113**, 2252–2257 (2016).
- 794 31. Oh, E. *et al.* Selective Ribosome Profiling Reveals the Cotranslational Chaperone Action of
795 Trigger Factor In Vivo. *Cell* **147**, 1295–1308 (2011).
- 796 32. Reck, M. *et al.* Stool metatranscriptomics: A technical guideline for mRNA stabilisation and
797 isolation. *BMC Genomics* **16**, 494 (2015).
- 798 33. Latif, H. *et al.* A streamlined ribosome profiling protocol for the characterization of
799 microorganisms. *BioTechniques* **58**, 329–332 (2015).

- 800 34. Bag, S. *et al.* An Improved Method for High Quality Metagenomics DNA Extraction from
801 Human and Environmental Samples. *Sci. Rep.* **6**, 26775 (2016).
- 802 35. Conditions for ethanol precipitation of active 50 S ribosomal subunits from *Escherichia coli* -
803 ScienceDirect. Available at:
804 <https://www.sciencedirect.com/science/article/pii/S09266410171372>. (Accessed: 15th April
805 2018)
- 806 36. Tamburini, F. B. *et al.* Precision Identification of Diverse Bloodstream Pathogens from the
807 Gut Microbiome. *bioRxiv* 310441 (2018). doi:10.1101/310441
- 808 37. Maier, T., Güell, M. & Serrano, L. Correlation of mRNA and protein in complex biological
809 samples. *FEBS Lett.* **583**, 3966–3973 (2009).
- 810 38. Hyatt, D. *et al.* Prodigal: prokaryotic gene recognition and translation initiation site
811 identification. *BMC Bioinformatics* **11**, 119 (2010).
- 812 39. Washietl, S. *et al.* RNACode: Robust discrimination of coding and noncoding regions in
813 comparative sequence data. *RNA* **17**, 578–594 (2011).
- 814 40. Götz, S. *et al.* High-throughput functional annotation and data mining with the Blast2GO
815 suite. *Nucleic Acids Res.* **36**, 3420–3435 (2008).
- 816 41. Seemann, T. Prokka: rapid prokaryotic genome annotation. *Bioinforma. Oxf. Engl.* **30**, 2068–
817 2069 (2014).
- 818 42. Ndah, E. *et al.* REPARATION: Ribosome Profiling Assisted (Re-)Annotation of Bacterial
819 genomes. *bioRxiv* 113530 (2017). doi:10.1101/113530
- 820 43. Wiśniewski, J. R., Zougman, A., Nagaraj, N. & Mann, M. Universal sample preparation
821 method for proteome analysis. *Nat. Methods* **6**, 359–362 (2009).

- 822 44. Tanca, A. *et al.* A straightforward and efficient analytical pipeline for metaproteome
823 characterization. *Microbiome* **2**, 49 (2014).
- 824 45. Bern, M., Kil, Y. J. & Becker, C. Byonic: Advanced Peptide and Protein Identification
825 Software. *Curr. Protoc. Bioinforma. Ed. Board Andreas Baxevanis Al* **CHAPTER**,
826 Unit13.20 (2012).
- 827 46. Nurk, S. *et al.* Assembling Genomes and Mini-metagenomes from Highly Chimeric Reads.
828 in *Research in Computational Molecular Biology* 158–170 (Springer, Berlin, Heidelberg,
829 2013). doi:10.1007/978-3-642-37195-0_13
- 830 47. Martin, M. Cutadapt removes adapter sequences from high-throughput sequencing reads.
831 *EMBnet.journal* **17**, 10–12 (2011).
- 832 48. Langmead, B., Trapnell, C., Pop, M. & Salzberg, S. L. Ultrafast and memory-efficient
833 alignment of short DNA sequences to the human genome. *Genome Biol.* **10**, R25 (2009).
- 834 49. Robinson, J. T. *et al.* Integrative genomics viewer. *Nat. Biotechnol.* **29**, 24–26 (2011).
- 835 50. Madden, T. *The BLAST Sequence Analysis Tool*. (National Center for Biotechnology
836 Information (US), 2003).
- 837 51. Laslett, D. & Canback, B. ARAGORN, a program to detect tRNA genes and tmRNA genes
838 in nucleotide sequences. *Nucleic Acids Res.* **32**, 11–16 (2004).
- 839 52. Finn, R. D., Clements, J. & Eddy, S. R. HMMER web server: interactive sequence similarity
840 searching. *Nucleic Acids Res.* **39**, W29–W37 (2011).
- 841 53. riboSeqR. *Bioconductor* Available at: <http://bioconductor.org/packages/riboSeqR/>.
842 (Accessed: 28th February 2017)
- 843 54. Minot, S. S., Krumm, N. & Greenfield, N. B. One Codex: A Sensitive and Accurate Data
844 Platform for Genomic Microbial Identification. *bioRxiv* 027607 (2015). doi:10.1101/027607

- 845 55. Quinlan, A. R. & Hall, I. M. BEDTools: a flexible suite of utilities for comparing genomic
846 features. *Bioinforma. Oxf. Engl.* **26**, 841–842 (2010).
- 847 56. Love, M. I., Huber, W. & Anders, S. Moderated estimation of fold change and dispersion for
848 RNA-seq data with DESeq2. *Genome Biol.* **15**, 550 (2014).
- 849 57. Warnes, G. R. *et al.* *gplots: Various R Programming Tools for Plotting Data.* (2016).
- 850 58. Jr, F. E. H. & others, with contributions from C. D. and many. *Hmisc: Harrell*
851 *Miscellaneous.* (2018).
- 852 59. Wickham, H., Chang, W. & RStudio. *ggplot2: Create Elegant Data Visualisations Using the*
853 *Grammar of Graphics.* (2016).
- 854 60. Diedenhofen, B. *cocor: Comparing Correlations.* (2016).
- 855 61. Zou, G. Y. Toward using confidence intervals to compare correlations. *Psychol. Methods* **12**,
856 399–413 (2007).
- 857 62. Li, W. & Godzik, A. Cd-hit: a fast program for clustering and comparing large sets of protein
858 or nucleotide sequences. *Bioinformatics* **22**, 1658–1659 (2006).
- 859 63. Bateman, A. *et al.* UniProt: the universal protein knowledgebase. *Nucleic Acids Res.* **45**,
860 D158–D169 (2017).
- 861 64. Huang, D. W., Sherman, B. T. & Lempicki, R. A. Systematic and integrative analysis of
862 large gene lists using DAVID bioinformatics resources. *Nat. Protoc.* **4**, 44–57 (2009).
- 863 65. Huang, D. W., Sherman, B. T. & Lempicki, R. A. Bioinformatics enrichment tools: paths
864 toward the comprehensive functional analysis of large gene lists. *Nucleic Acids Res.* **37**, 1–13
865 (2009).

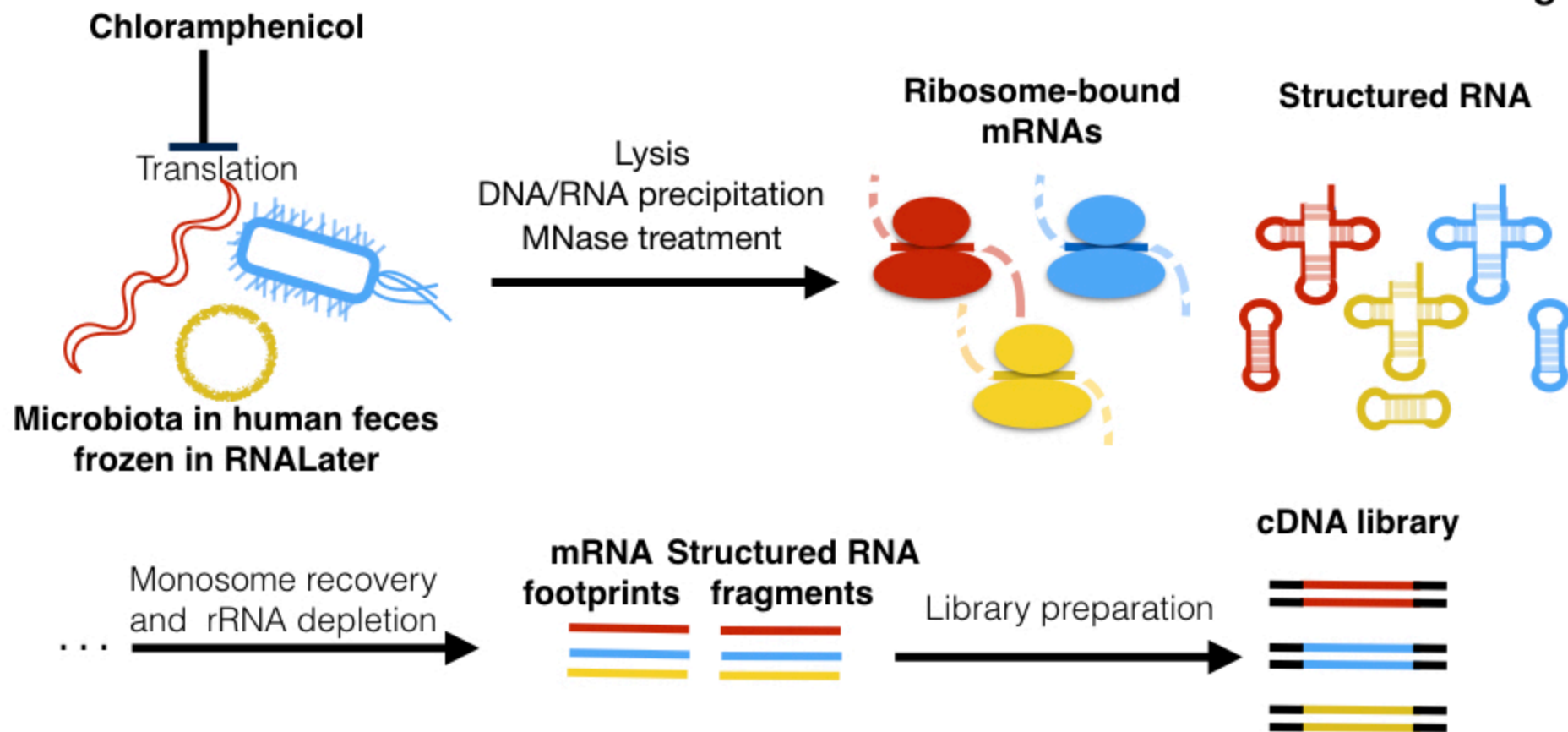
866 66. Dhariwal, A. *et al.* MicrobiomeAnalyst: a web-based tool for comprehensive statistical,
867 visual and meta-analysis of microbiome data. *Nucleic Acids Res.* (2017).

868 doi:10.1093/nar/gkx295

869

Figure 1

A



B

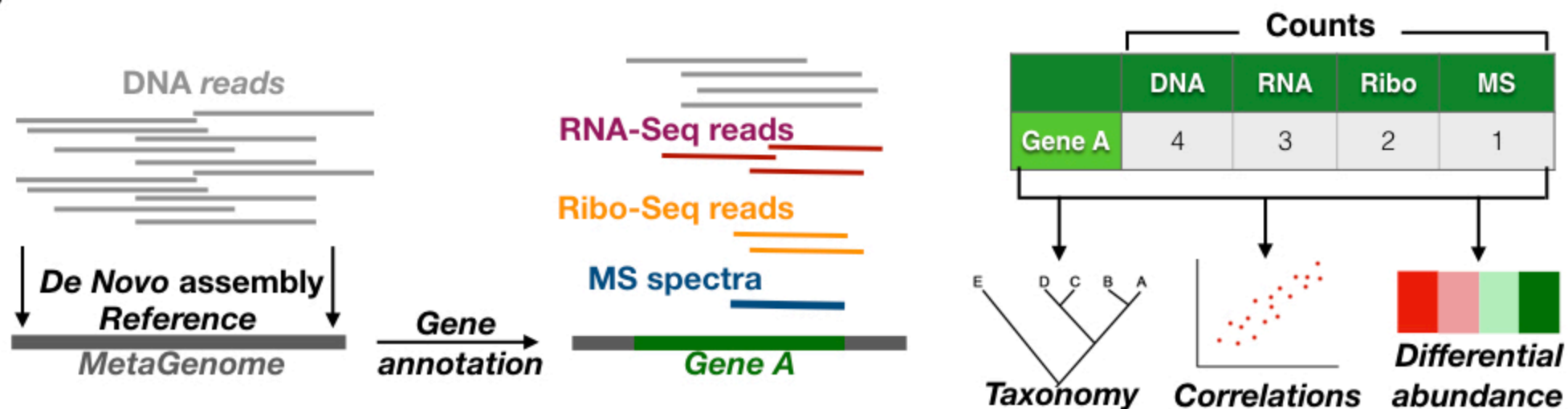


Figure 2

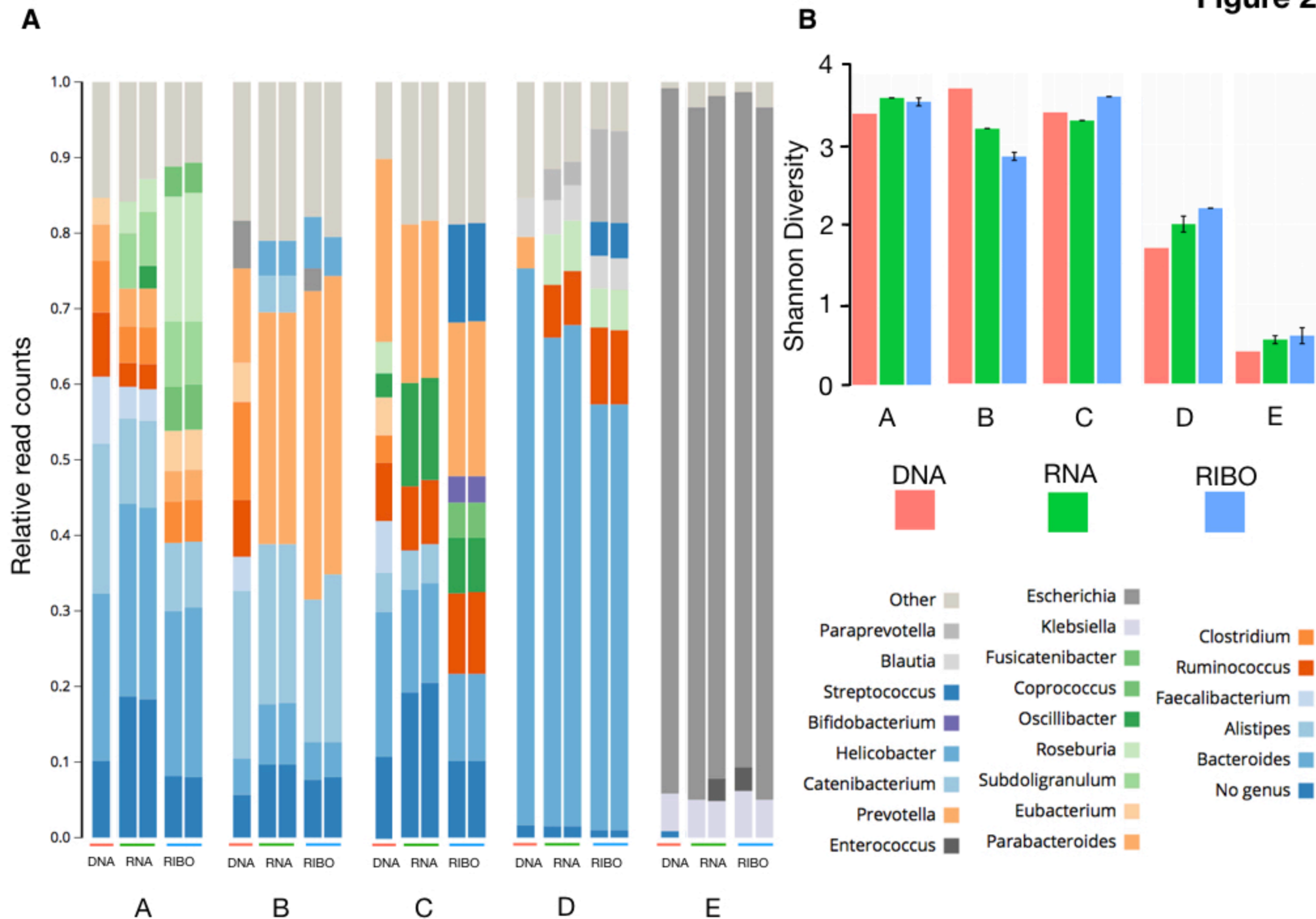
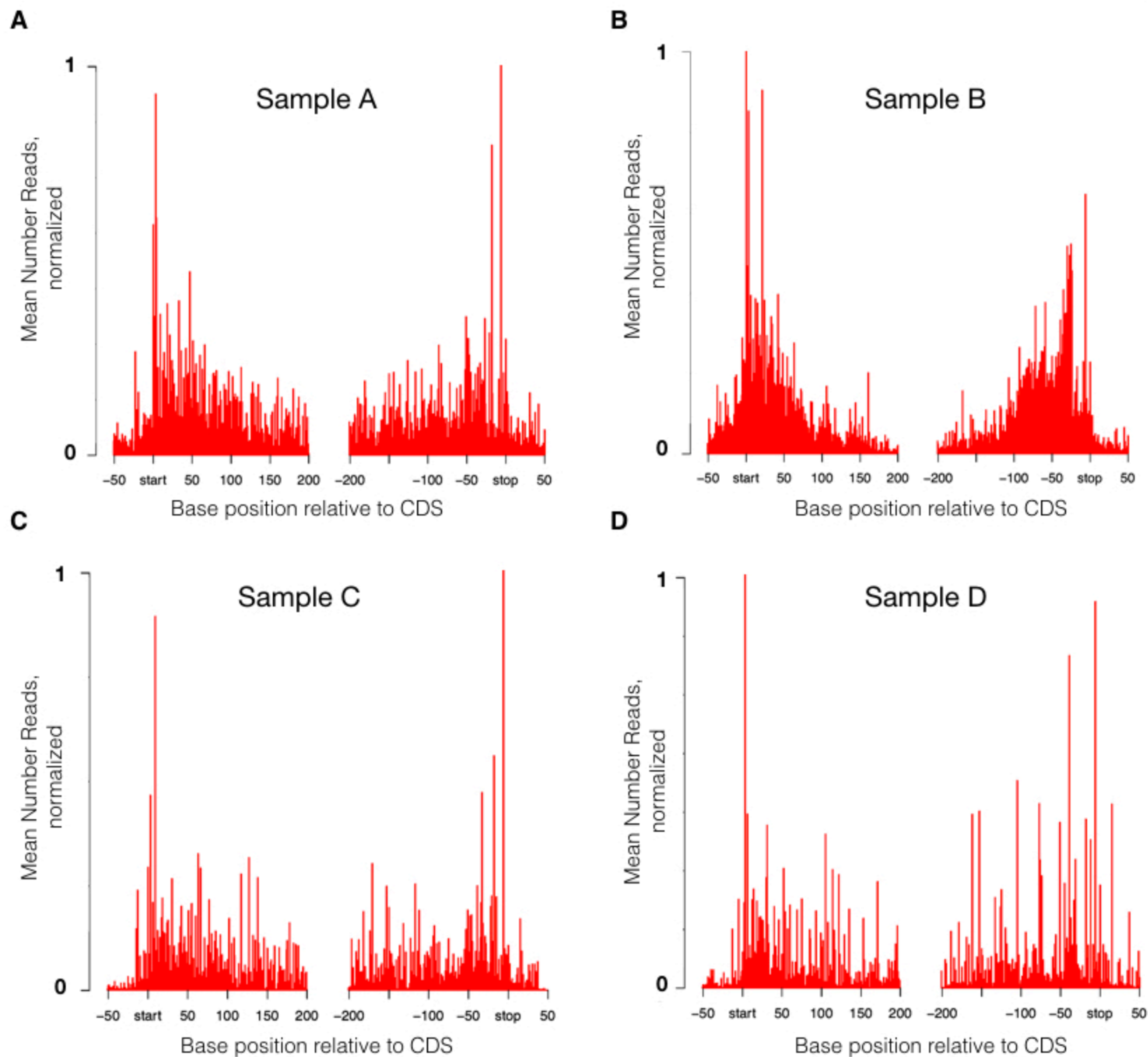


Figure 3



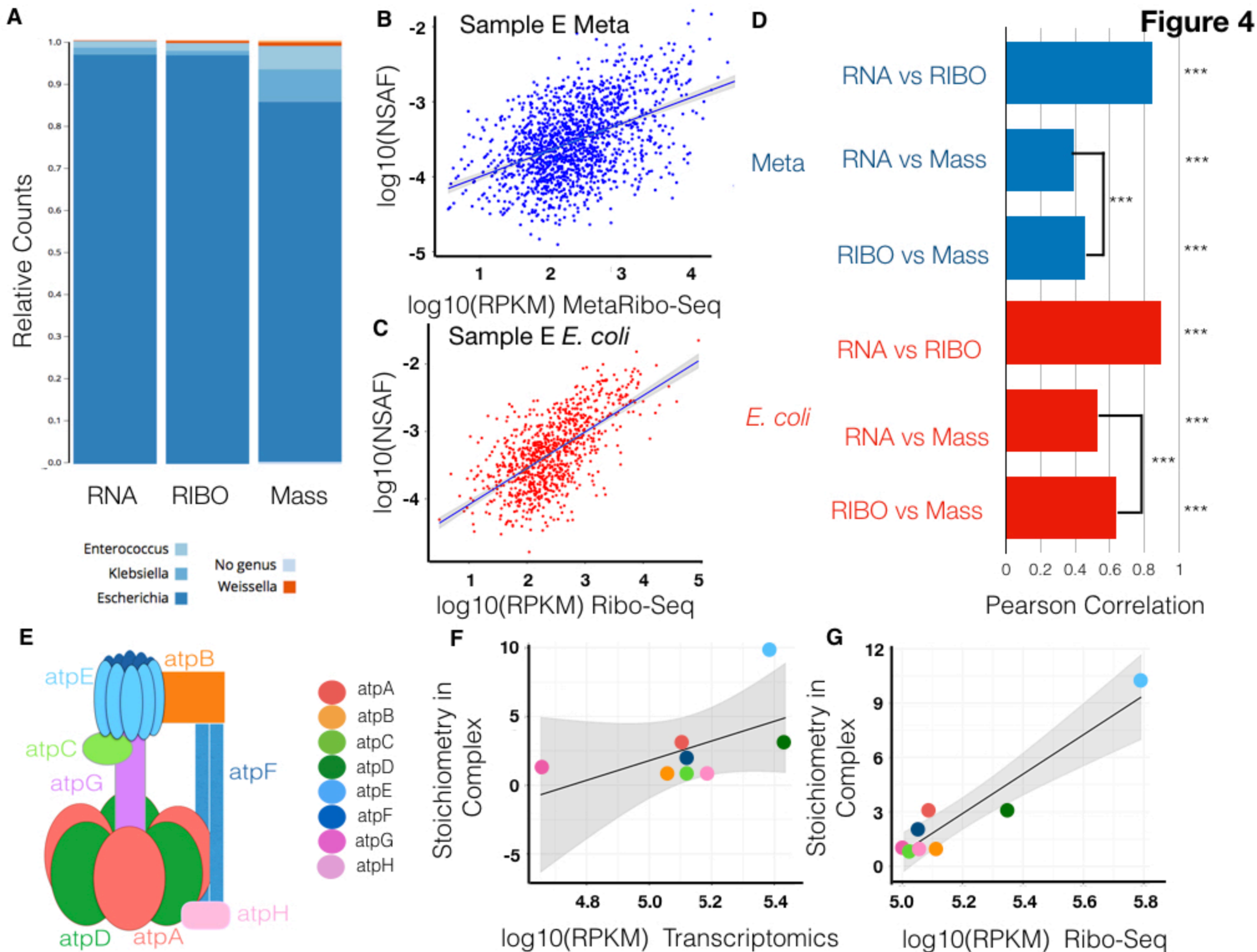


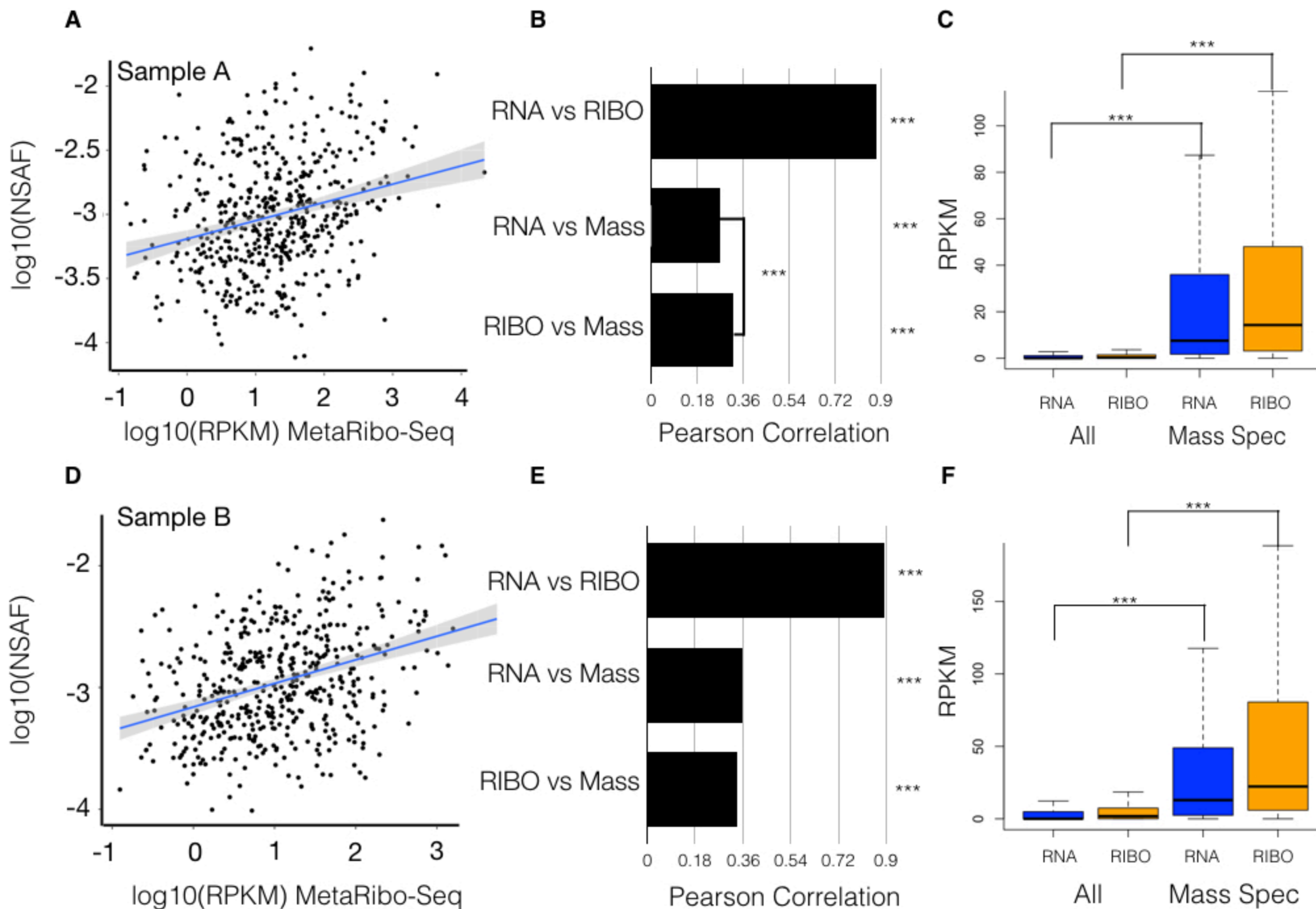
Figure 5

Figure 6

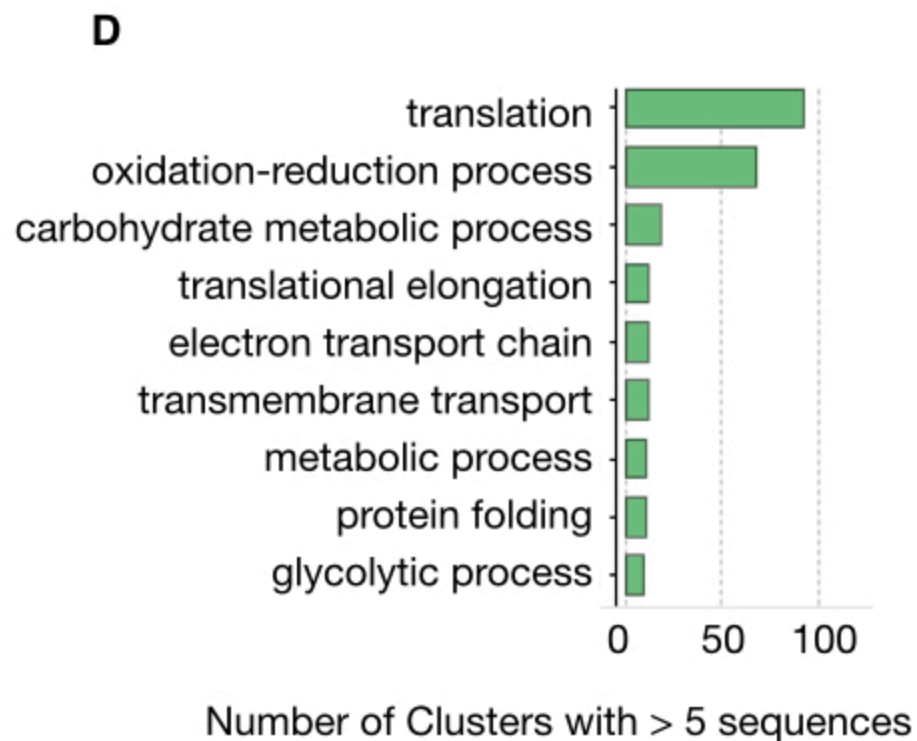
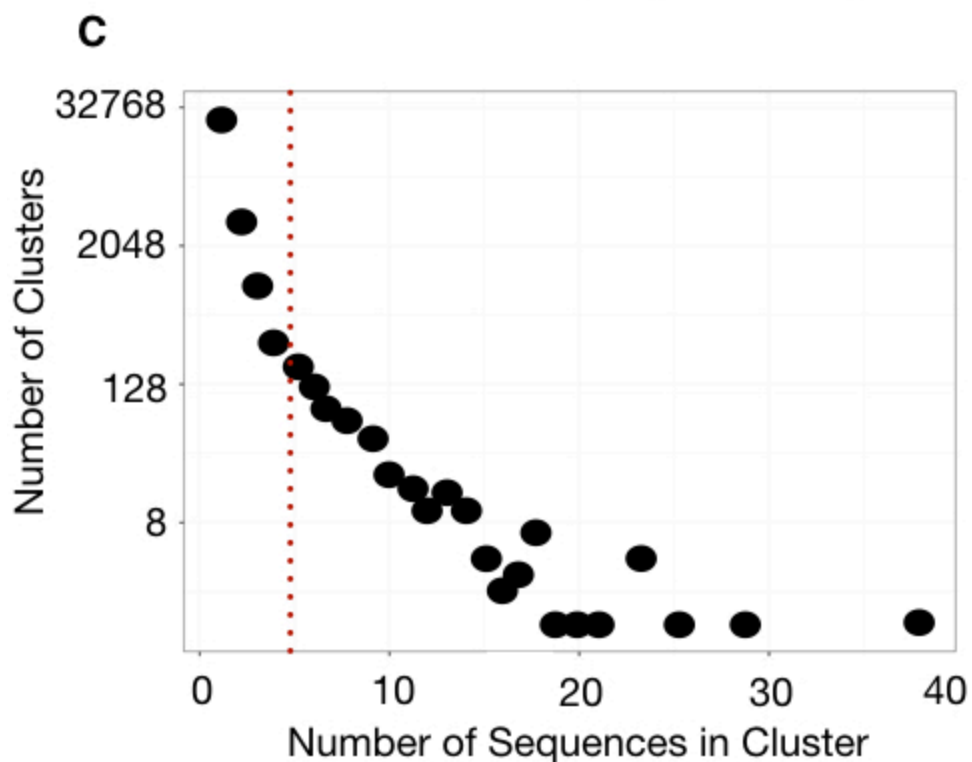
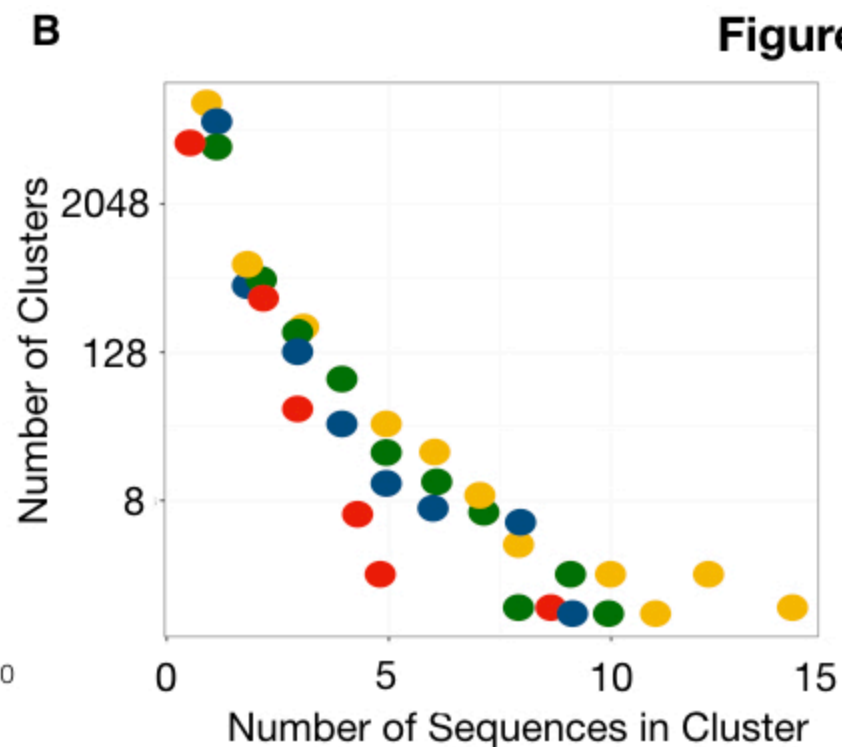
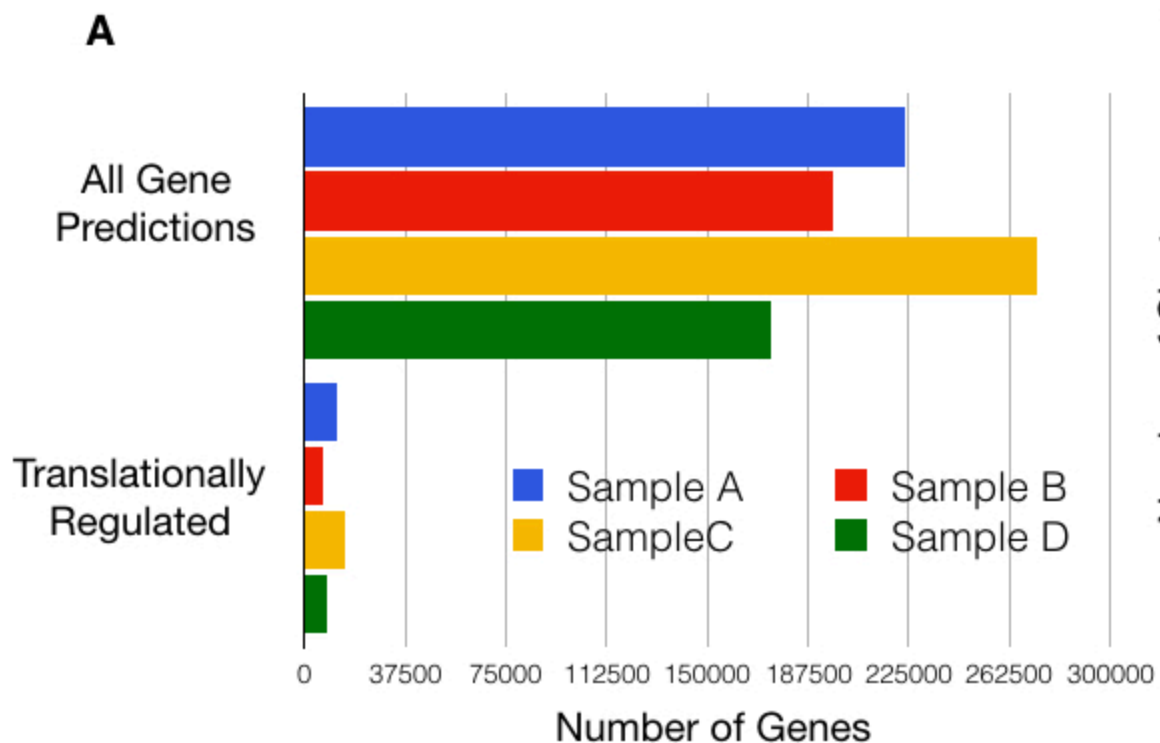
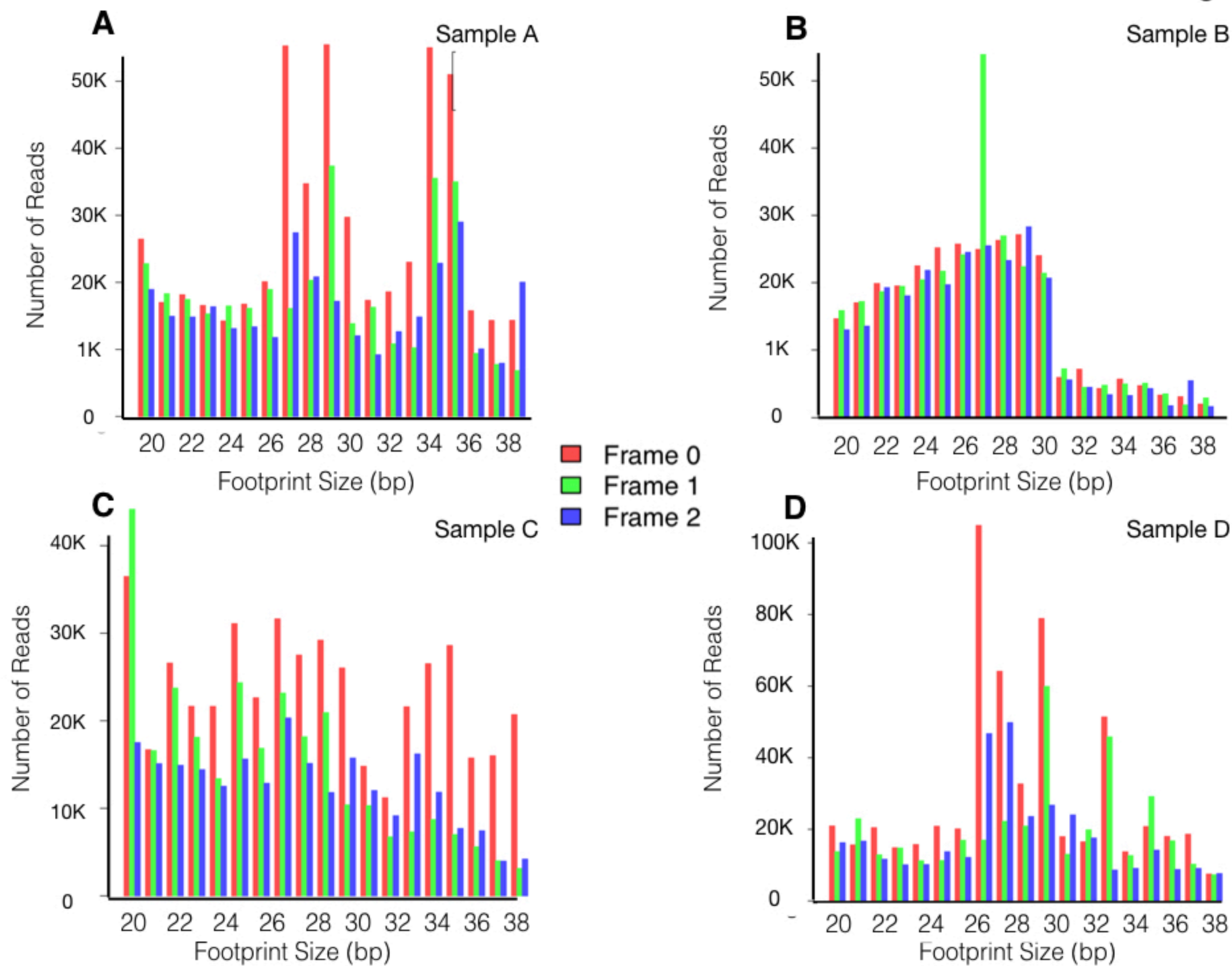
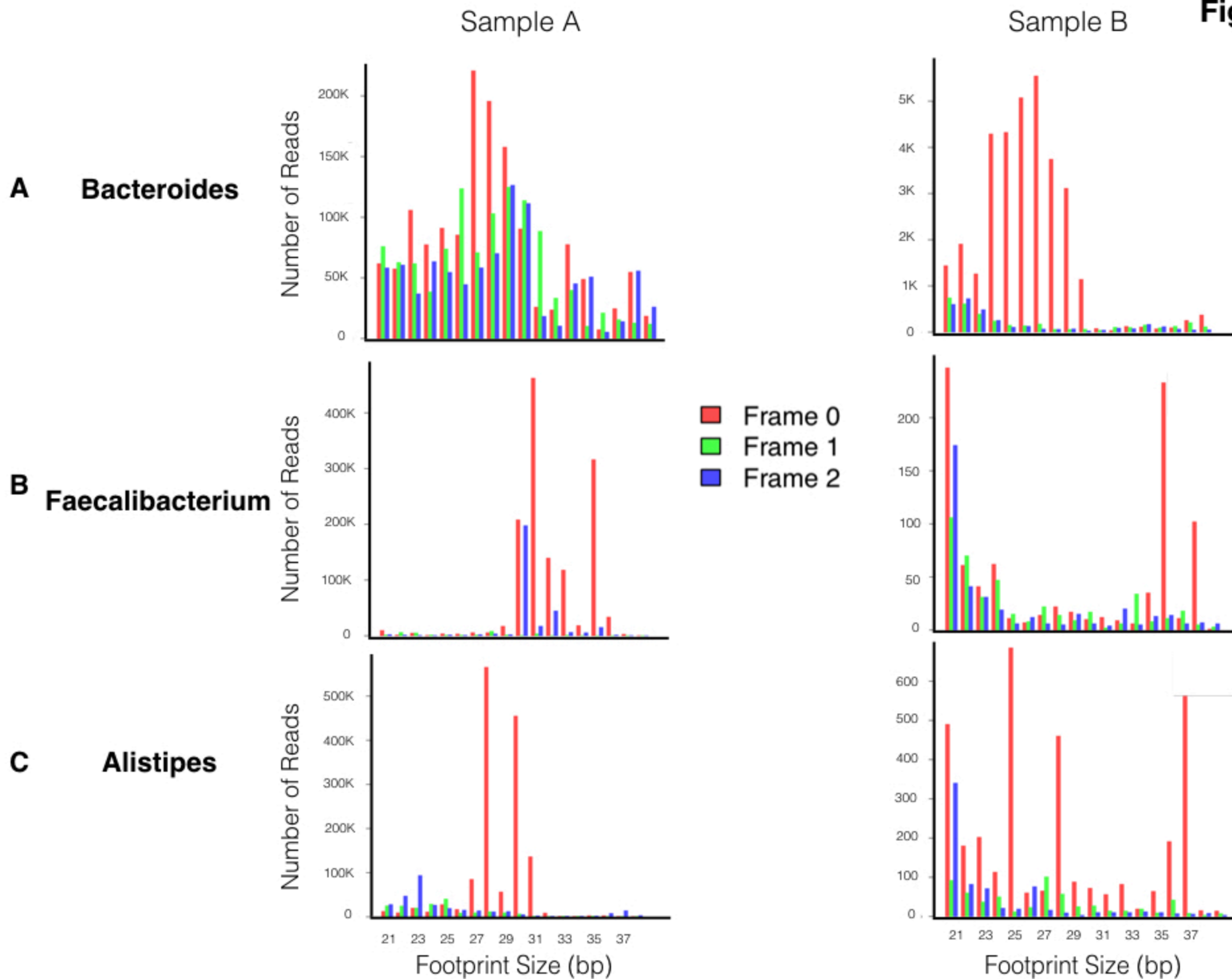
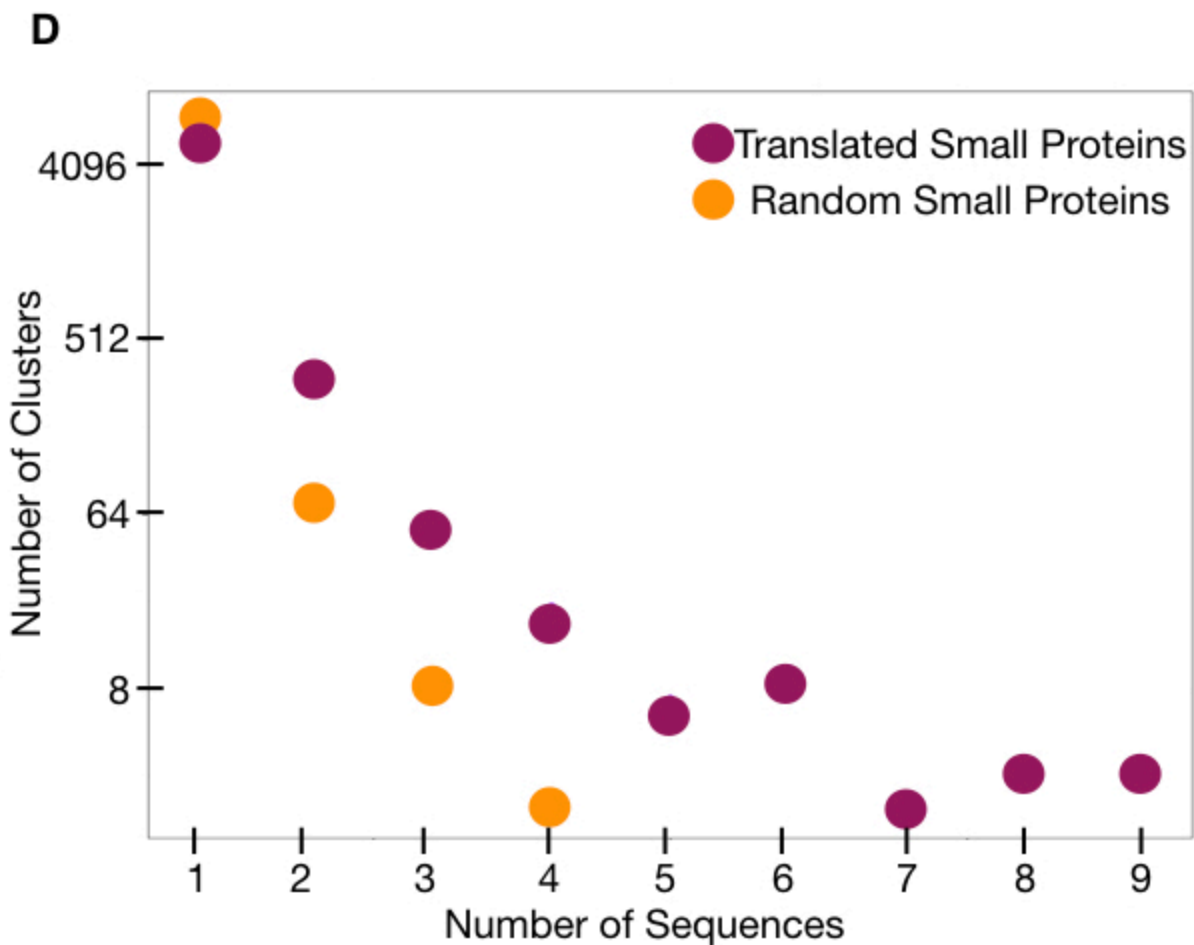
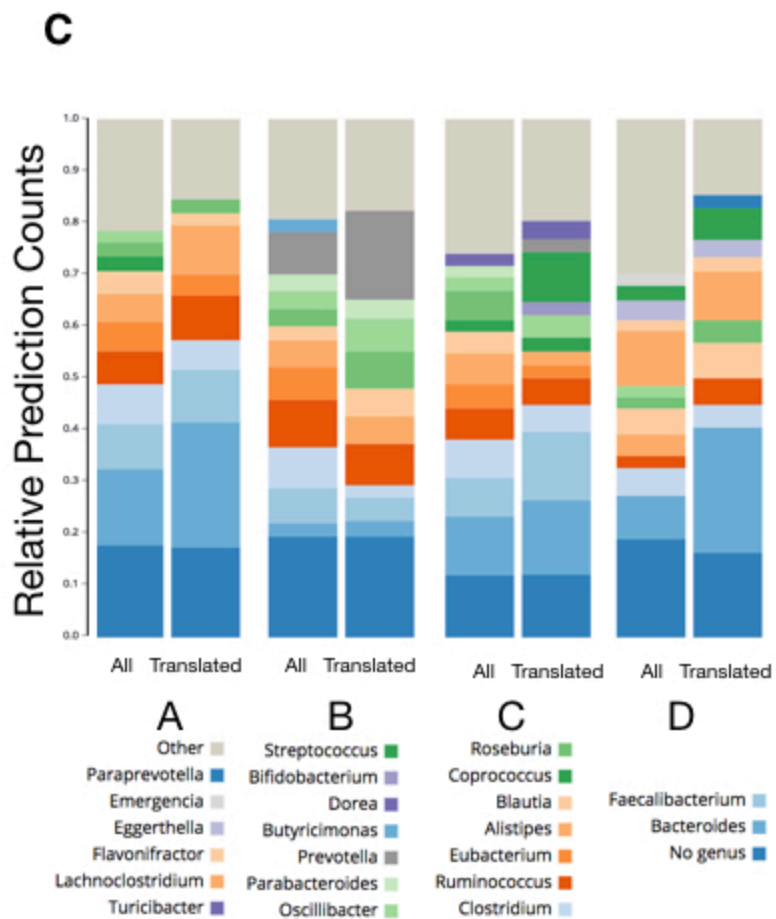
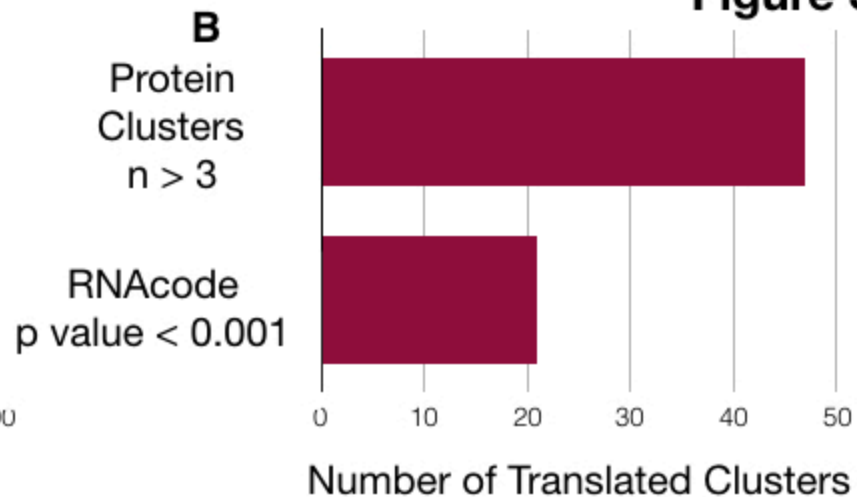
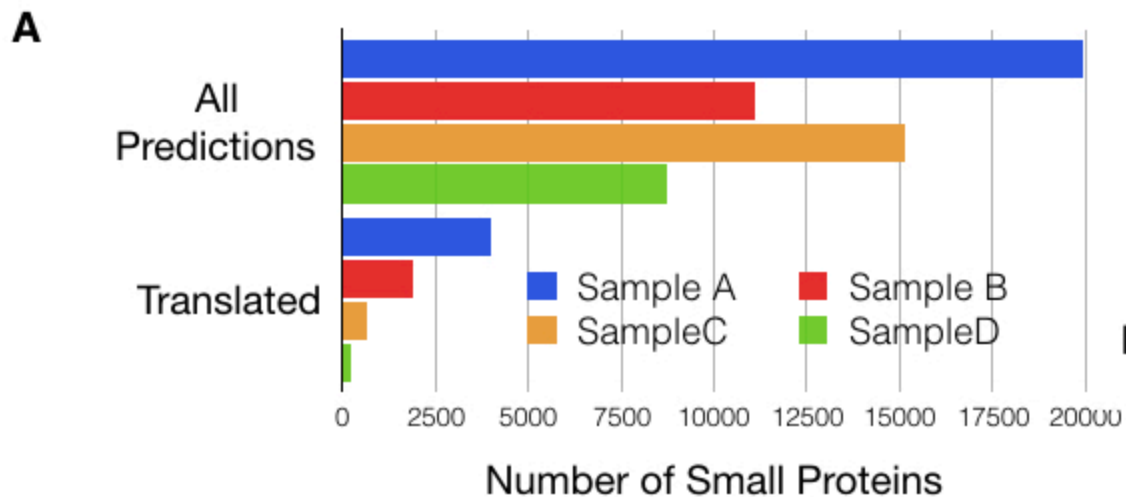
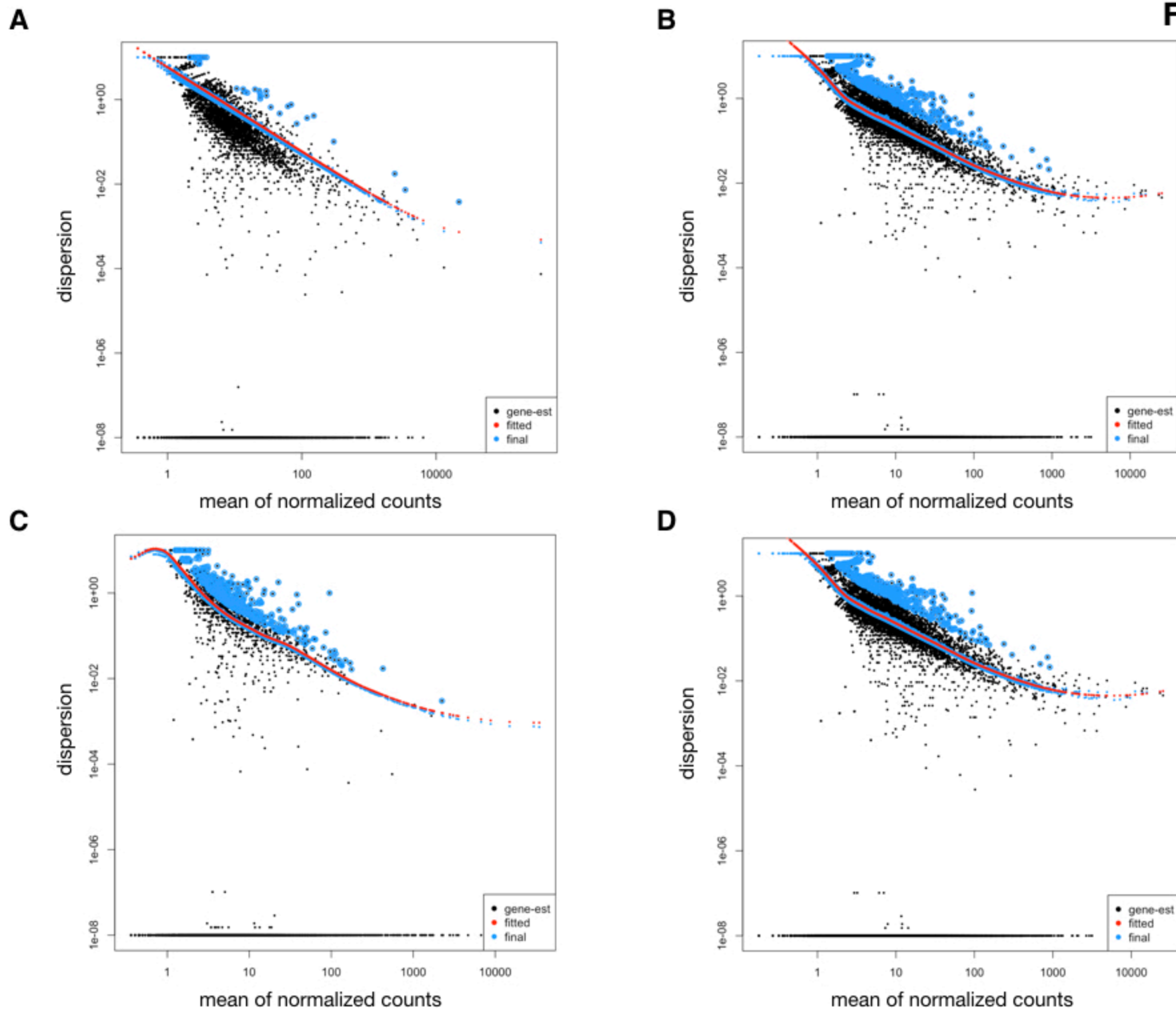


Figure S1







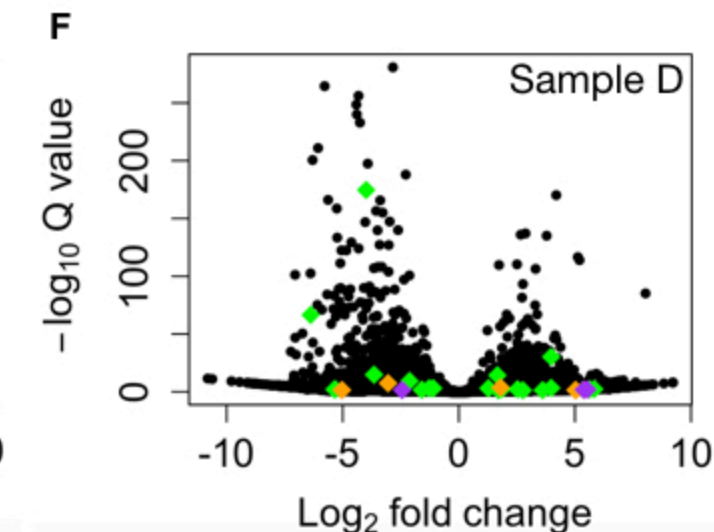
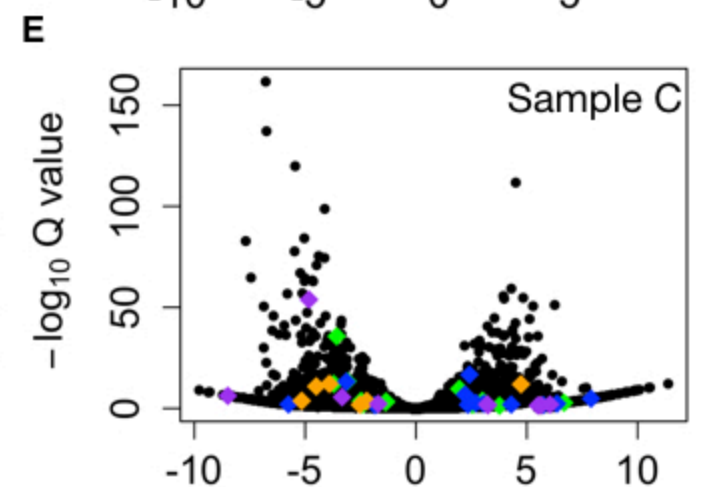
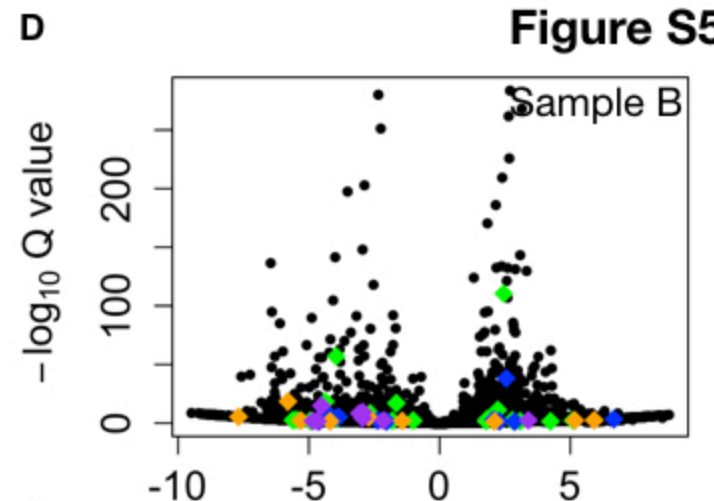
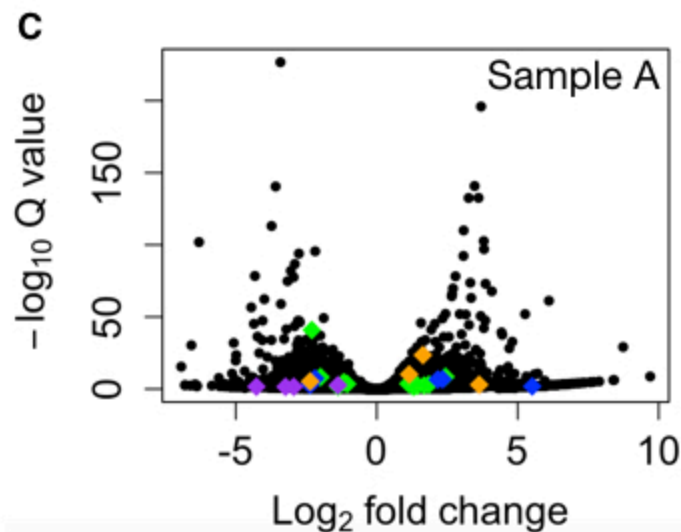
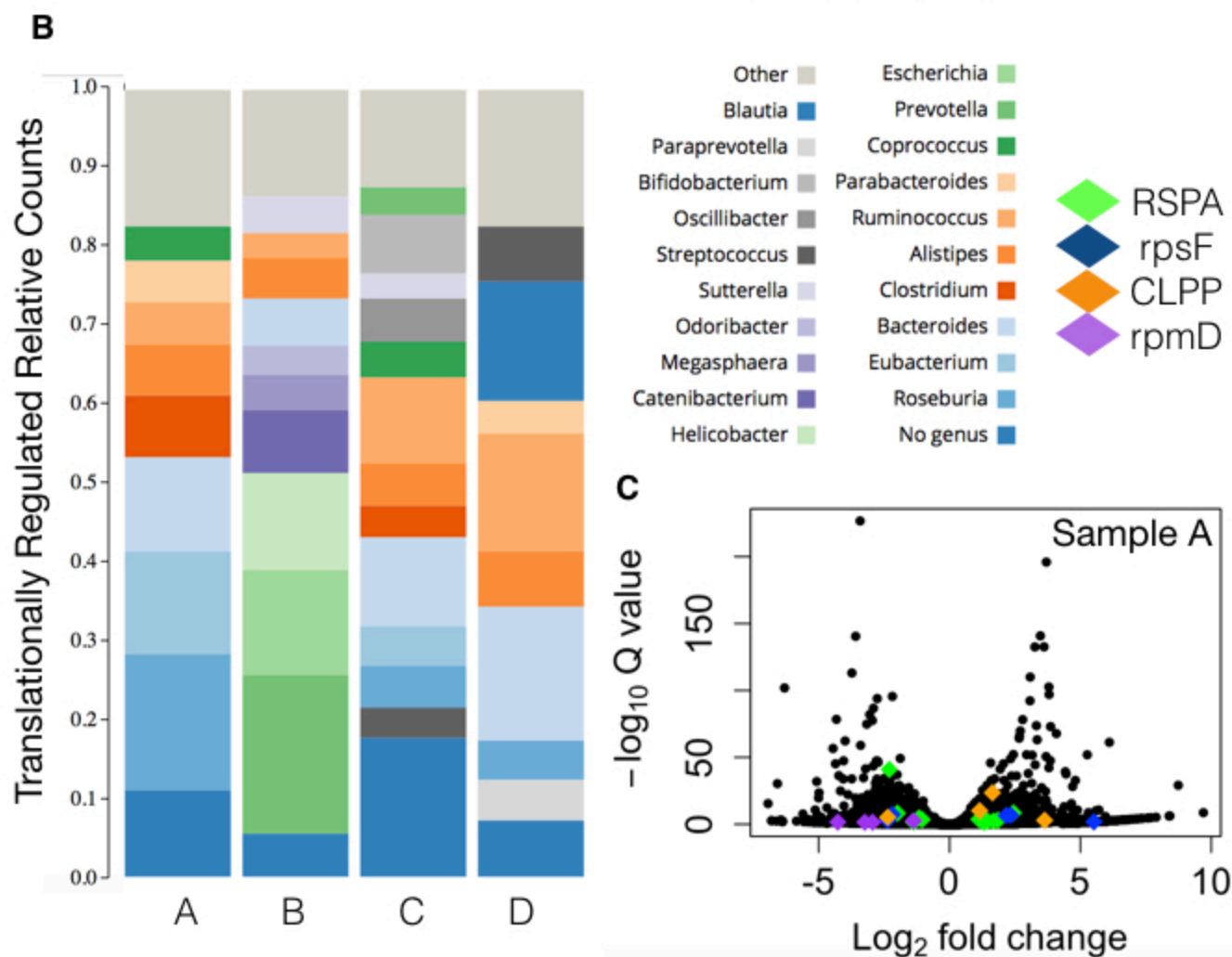
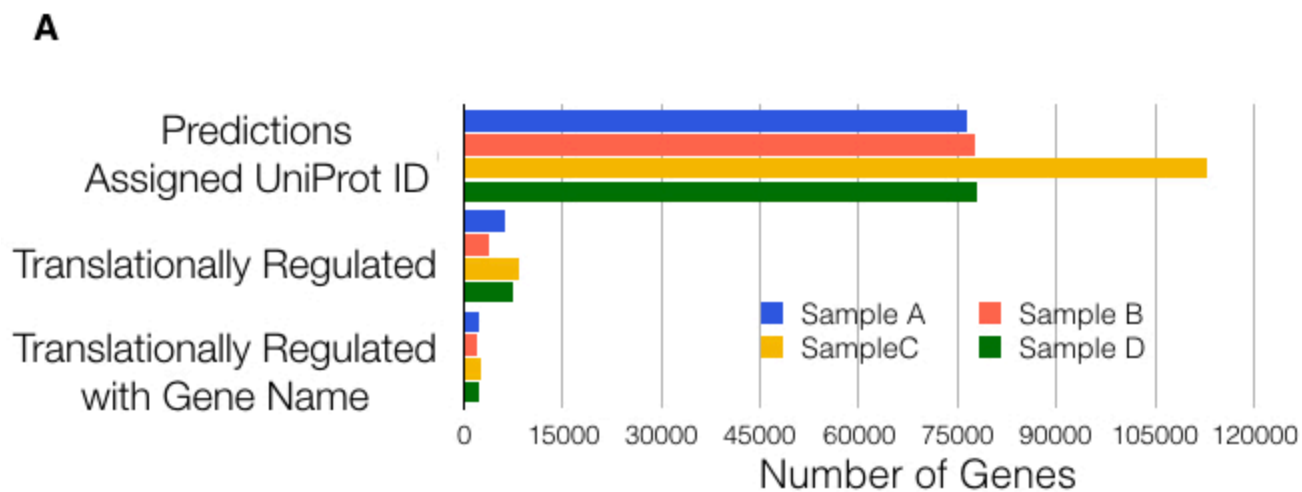
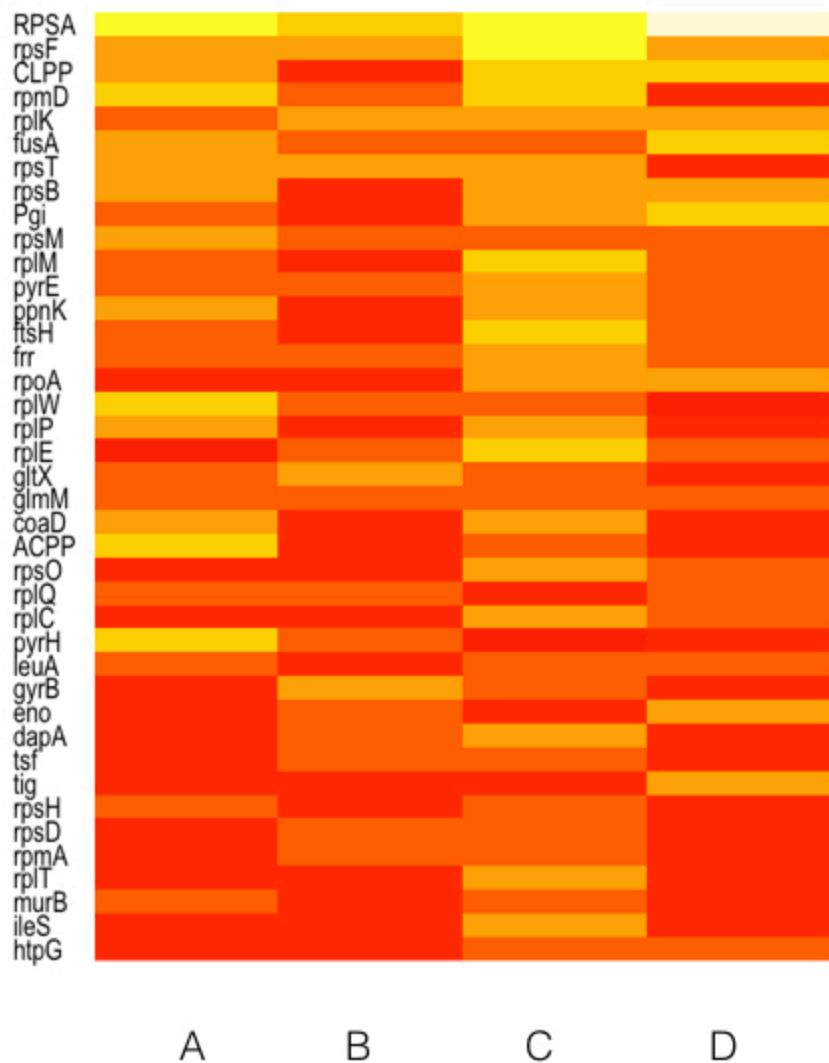


Figure S6

A



B

